Interaction of the C2C12 myotube contractions and glucose availability on transcriptome and extracellular vesicle microRNAs

Juulia H. Lautaoja-Kivipelto[1,2]*, Sira Karvinen[1], Tia-Marje Korhonen[1], Thomas M. O´Connell[3], Marja Tiirola[4], Juha J. Hulmi[1] & Satu Pekkala[1]

[1]Faculty of Sport and Health Sciences, NeuroMuscular Research Center, University of Jyväskylä, Jyväskylä, 40014, Finland; sira.m.karvinen@jyu.fi; tia-marje.k.korhonen@jyu.fi; juha.hulmi@jyu.fi; satu.p.pekkala@jyu.fi

[2]Faculty of Medicine, Research Unit of Biomedicine and Internal Medicine, University of Oulu, Oulu, 90014, Finland: juulia.lautaoja@oulu.fi

[3]Department of Otolaryngology-Head & Neck Surgery, Indiana University School of Medicine, Indianapolis, Indiana, 46202, United States; thoconne@iu.edu

[4]Department of Biological and Environmental Science, Nanoscience Center, University of Jyväskylä, Jyväskylä, 40014, Finland; marja.tiirola@jyu.fi

Keywords: electrical pulse stimulation, exercise, exerkine, skeletal muscle

Running head: Omics of the contracting C2C12 myotubes

*Correspondence: Juulia H. Lautaoja-Kivipelto: juulia.lautaoja@oulu.fi (ORCID: 0000-0003-2037-829X) Faculty of Sport and Health Sciences, NeuroMuscular Research Center, University of Jyväskylä, Jyväskylä, Finland and Faculty of Medicine, Research Unit of Biomedicine and Internal Medicine, University of Oulu, Oulu, Finland.

Supplemental Material available at:
Figure S1:
URL: https://figshare.com/s/b82719d36229d6a241d0
DOI: https://doi.org/10.6084/m9.figshare.23918376
Figure S2:
URL: https://figshare.com/s/72e6eade83a688d7012f

DOI: https://doi.org/10.6084/m9.figshare.23918415
Table S1:
URL: https://figshare.com/s/b481cf99bc5dfe1f283d
DOI: https://doi.org/10.6084/m9.figshare.23918385
Table S2:
URL: https://figshare.com/s/3105dca76c68d1563ca7
DOI: https://doi.org/10.6084/m9.figshare.24476524
Table S3:
URL: https://figshare.com/s/0e6f57c723e13de89b27
DOI: https://doi.org/10.6084/m9.figshare.23918475
Table S4:
URL: https://figshare.com/s/ea20ef3da4f131b0a0d3
DOI: https://doi.org/10.6084/m9.figshare.23931369
Table S5:
URL: https://figshare.com/s/4a1f3658fff4dbb8be6a
DOI: https://doi.org/10.6084/m9.figshare.23931375

ABSTRACT

Exercise-like electrical pulse stimulation (EL-EPS) of myotubes mimics many key physiological changes induced by *in vivo* exercise. Besides enabling intracellular research, EL-EPS allows to study secreted factors, including muscle-specific microRNAs (myomiRs) carried in extracellular vesicles (EVs). These factors can participate in contraction-induced intercellular crosstalk and may mediate health benefits of exercise. However, the current knowledge of these responses, especially under variable nutritional conditions, is limited. We investigated the effects of EL-EPS on C2C12 myotube transcriptome in high and low glucose conditions by messenger RNA sequencing, while the expression of EV-carried miRNAs was analyzed by small RNA sequencing and RT-qPCR. We show that higher glucose availability augmented contraction-induced transcriptional changes and that the majority of the differentially expressed genes were upregulated. Furthermore, based on the pathway analyses, processes related to contractility and cytokine/inflammatory responses were upregulated. Additionally, we report that EL-EPS increased packing of miR-1-3p into EVs independent of glucose availability. Together our findings suggest that *in vitro* EL-EPS is a usable tool not only to study contraction-induced intracellular mechanisms, but also extracellular responses. The distinct transcriptional changes observed under variable nutritional conditions emphasize the importance of careful consideration of media composition in future exercise-mimicking studies.

NEW & NOTEWORTHY

The present study examined for the first time the effects of exercise-like electrical pulse stimulation administered under distinct nutritional conditions on 1) the transcriptome of the C2C12 myotubes and 2) their media containing extracellular vesicle-carried microRNAs. We report that higher glucose availability augmented transcriptional responses related especially to contractility and cytokine/inflammatory pathways. Agreeing with *in vivo* studies, we show that packing of exercise-responsive miR-1-3p was increased in the extracellular vesicles in response to myotube contractions.

INTRODUCTION

Exercise is known to promote health as well as to ameliorate and treat many diseases caused by sedentary lifestyle and obesity (1). During exercise skeletal muscles can modify not just their own, but also the metabolism of other organs, such as liver and adipose tissue (2). Exerkines are molecules released in response to acute and/or chronic exercise exerting their effects through endocrine, paracrine and/or autocrine pathways (3). Many organs including skeletal muscle produce and release these exerkines, such as proteins/peptides, cytokines, nucleic acids, metabolites as well as extracellular vesicles (EVs), and release them into circulation in response to exercise (2, 4). Numerous *in vivo* and *in vitro* studies have identified and validated various exerkines as well as some of their functions and target tissues (for review, see (2, 3)). Previous studies have shown that skeletal muscle specific exercise-like electrical pulse stimulation (EL-EPS) (5) of the myotubes can mimic many intra- and extracellular responses of *in vivo* exercise at the cellular (5, 6) and omics (7) levels. Additionally, we have previously shown that media glucose availability altered the metabolic responses of the C2C12 myotubes to EL-EPS (8). Because myotube gene expression is significantly impacted by the media glucose content (9, 10) and exercise responses have been reported to be affected by carbohydrate availability *in vivo* (11), it is important to examine how EL-EPS together with the variable nutritional conditions affects myotube transcriptome and regulation of the expression of genes encoding, for example, different exerkines.

Accumulating evidence demonstrates that EVs can encapsulate exerkines and transmit this functional cargo, such as microRNAs (miRNAs) (12, 13), via circulation to nearby and/or distant organs and tissues (14). We (15) and others (16) have shown that acute exercise induces changes in the miRNA cargo of EVs. Furthermore, some of the health-beneficial effects and adaptations of exercise have been reported to be mediated by miRNAs (17), thus making them an appealing target for biomarker research. Previous studies have shown that the levels of muscle-specific miRNAs, i.e., myomiRs, such as miR-1, miR-133a, and miR-206, are increased in the circulating EVs after exercise (12, 13). EVs are a heterogeneous group of membrane-bound particles found virtually from all biofluids *in vivo* and from conditioned cell culture media *in vitro* (17). Because the EV content can vary depending on the physiological state of the cells from which they

originate (18), it is important to study how nutrient availability affects EV-mediated intercellular crosstalk in response to myotube contractions. Additionally, *in vitro* approaches are needed to study the myotube-derived EVs because *in vivo* models cannot exclude the possibility that the EVs collected from the circulation, even in the presence of certain predetermined markers, are not of muscular origin.

This study aimed to analyze the effects of the chronic low-frequency EL-EPS together with varying media glucose content on the C2C12 myotube transcriptome and EV cargo. Several bioinformatic analyses were used to reveal the underlying mechanisms through which EL-EPS and/or availability of nutrients affect physiological responses and related pathways.

MATERIAL AND METHODS

Cell culture. The murine C2C12 myoblasts purchased from American Type Culture Collection (Manassas, VA, USA) were grown and differentiated identically as previously described in detail (8). Briefly, the myoblasts were seeded on 6-well plates and grown in high glucose (HG, 4.5 g/l, #BE12-614F, Lonza, Basel, Switzerland) containing growth medium. After reaching over 90% confluence, the fusion into myotubes was promoted by HG-containing differentiation medium (DM) (8). Representative images of the C2C12 myotubes differentiated with the identical protocol have been published previously elsewhere by us (19). The media volume per well during differentiation and experiments was 2 ml. All the experiments were performed using cells with passage number between 6-8 in a humidified environment at 37°C and 5% CO_2.

Exercise-like electrical pulse stimulation. The experiments were conducted on days 4-6 post myotube differentiation by using either high or low glucose (LG, 1 g/l, #BE12-707F, Lonza) DMEM identically as previously described (8) (Figure 1). Briefly, if LG medium was used, the cells were acclimatized to LG DM from day 4 post differentiation. At day 5 post differentiation, serum- and antibiotic-free HG or LG DMEM supplemented with 2 mM L-glutamine (#25030, Gibco, Rockville, MD, USA) was added for 1 hour (20). Serum-free conditions are important not only to exclude the effects of switching to serum-free medium (20), but also to avoid co-isolation of exogenous EVs or other signal carrier particles, such as high-density lipoproteins (21). Next, the medium was removed, the myotubes were rinsed with phosphate-buffered saline (PBS, #10010, Gibco), and fresh serum-free HG or LG DMEM supplemented with 2 mM L-glutamine was added. The low-frequency EL-EPS was applied for 24 hours (1 Hz, 2 ms, 12 V) using C-Dish carbon electrodes attached to C-Pace device (Ionoptix Corporation, Milton, MA, USA). Carbon electrodes that were not attached to the C-Pace device were also placed on the control plates for the EV extraction experiments (sRNA-seq). This was done to exclude the effects of the electrodes on the EV extraction because EVs have high affinity to different types of surfaces, at least plastic (22). On day 6 post differentiation, the samples were harvested immediately after cessation of EL-EPS. To remove cell debris, media were centrifuged for 5 min at 382 x g at 4˚C and the supernatants were stored at -80°C until EV extraction. Simultaneously, the myotubes

were washed with PBS, scraped into 340 µl of DNA/RNA Shield (#R1100, Zymo Research, Irvine, CA, USA) and stored at room temperature (RT) until total RNA extraction.

Validation of the EV isolation by nanoparticle tracking analysis and electron microscopy. The EVs were isolated using exoRNeasy serum/plasma midi kit (#77044, Qiagen, Hilden, Germany) as previously described (23). For the validation of the EV isolation protocol, 1.5 ml of media was used. Briefly, EVs were eluted by adding 140 µl of elution buffer XE (#76214, Qiagen) followed by 5 min incubation and centrifugation for 5 min at 500 x g at RT. The collected eluate was then mixed with 360 µl of PBS that was filtered through a 0.2 µm filter, transferred into a 100K ultra-filter device (UFC5100, Amicon, Millipore, Darmstadt, Germany), and centrifuged for 10 min at 14 000 x g at RT. Next, the EVs were washed three times with filtered PBS to purify EVs from possible debris originating from the affinity columns and the flow-through was discarded. The concentrate was recovered by centrifugation for 2 min at 1000 x g at RT according to the manufacturer´s protocol. The analyses of the particle size (nanoparticle tracking analysis) and morphology (electron microscopy) were conducted at the University of Helsinki EV core (Helsinki, Finland) as previously described (23, 24). Low protein binding tubes were used whenever possible during the EV sample collection and purification.

RNA extraction. Nucleic acid extraction from the C2C12 myotube lysates stored in the DNA/RNA Shield (Zymo Research) was conducted using Chemagic 360 automated nucleic acid extraction instrument (Perkin Elmer, Boston, MA, USA). The total RNA extraction from the EVs was conducted using the exoRNeasy Serum/Plasma Midi Kit (#77144 or after discontinuation #77044, Qiagen) according to the manufacturer´s protocol. Briefly about the EV RNA extraction, media from two or three wells were pooled and run through the exoRNeasy spin columns. During the RNA extraction for RT-qPCR, miRNeasy Serum/Plasma Spike-In Control, cel-miR-39 (#219610, Qiagen) was added to be used as an internal control.

Library preparation and mRNA-sequencing. The total RNA samples of the cell lysates were first treated with dsDNase (EN0771, Thermo Scientific, Waltham, MA, USA) to eliminate genomic DNA. Then, RNA concentration and integrity were measured with TapeStation

(Agilent Technologies, Santa Clara, CA, USA) according to the manufacturer´s instructions. The average RNA integrity number (RIN) value was 8.97 ± 0.22 (standard error of mean) showing low degradation of RNA. The sequencing libraries for the gene expression profiling (3´ mRNA-seq) were prepared using a commercial kit (012.24A, QuantSeq 3′ mRNA-Seq Library Prep Kit for Ion Torrent, Lexogen, Inc., Vienna, Austria) according to the manufacturer´s protocols. After measuring the DNA concentrations with Qubit dsDNA HS Assay Kit (Invitrogen), the barcoded libraries were pooled in equimolar concentrations (5 ng of each). The pool was then purified with 1.2x sparQ PureMag Beads (QuantaBio, Beverly, MA, USA) and run on a High Sensitivity D1000 Screen Tape (Agilent Technologies) to determine the quality and molarity of the pool. To bind the template to the Ion Sphere Particles (ISPs), emulsion PCR was conducted in OneTouch2 instrument with Ion PGM™ Hi-Q™ OT2 Kit (Life Technologies, Carslbad, CA, USA) following the protocol for 400-bp template according to the manufacturer's instructions. The ISPs were loaded into an Ion 318 v2 BC chip and sequencing was performed in Ion Torrent Personal Genome Machine using Ion PGM™ Hi-Q™ View Sequencing Kit (Life Technologies) similarly as described previously by us (25). To obtain a similar amount of reads from all samples, the data were pooled from two 318 v2 chips.

Library preparation and small RNA-sequencing. After the EV RNA extraction, the RIN values were not measured as small RNA (sRNA) is less sensitive for degradation and as the RNA concentration was low. The small RNA libraries for the miRNA expression profiling (sRNA-seq) were prepared using a commercial kit (#4475936, Ion Total RNA-Seq Kit v2, 12 reaction kit, Thermo Fisher Scientific) according to the manufacturer´s protocols with slight modifications. The products were amplified using primer pair M13_IA 5´-TGTAAAACGACGGCCAGTGGCCAAGGCG-3´ and P1 5´-CCACTACGCCTCCGCTTT-3´ using the Platinum Supermix and for second time using the primer P1 and the IonA_bc_M13 adapter 5´-CCATCTCATCCCTGCGTGTCTCCGACTCAGXXXTGTAAAACGACGGCCAGT-3´, where XXX refers to the IonXpress barcode. The barcoded samples were pooled in equal volumes and 100-140 bp sized PCR products (including 92 bp of adapter sequences) were isolated using 1.6% NuSieve agarose (Lonza) gel electrophoresis and Nucleospin Gel and PCR Cleanup (Macherey-Nagel) extraction. From this step onwards, the sequencing protocol is identical with mRNA

protocol described above, except that the samples were sequenced using Ion GeneStudio™ S5 System with the 540 chip (Life Technologies).

cDNA synthesis and real-time quantitative PCR. For the RT-qPCR from the cell lysates, genomic DNA was eliminated, and the cDNA was synthetized using Maxima H first strand cDNA synthesis kit with dsDNase (#K1682, Thermo Fisher Scientific) according to the manufacturer´s protocol. The RT-qPCR was conducted as previously described (26). The efficiency-corrected $2^{-\Delta\Delta Ct}$ method was utilized for the RT-qPCR data analysis and *36b4* was the housekeeping gene used for normalization. The Bio-Rad Prime PCR™ Assays (Bio-Rad Laboratories, Hercules, CA, USA) used were as follows: *Cxcl1* (qMmuCED0003898), *Cxcl5* (qMmuCED0003886) and *Scml4* (qMmuCED0050877). The primer sequences for *36b4* were 5´-GGCCCTGCACTCTCGCTTTC-3´ and 5´- TGCCAGGACGCGCTTGT-3´ and for *Tceal7* 5´-TTGTGGCAAGGAGAAGAGAAG-3´ and 5´-TGAAATTGCCTTCCAGTCGC-3´. For the RT-qPCR from the EVs, the extracted total RNA was reverse transcribed by using 12 µl of the RNA and miScript II RT Kit (#218161, Qiagen) according to manufacturer´s instructions. The RT-qPCR was conducted as previously described for miRNAs and the data was analyzed by using the equation $2^{-\Delta Cq}$ (23). The spike-in control cel-miR-39-3p was used for normalization. The miScript Primer Assays (Qiagen) used in the RT-qPCR were miR-1-3p (MS00008358), miR-133a-3p (MS00031423) and cel-miR-39-3p (MS00019789). For miR-206-3p the miScript Primer Assay was not available, and hence it was ordered separately (sequence 5′-TGGAATGTAAGGAAGTGTGTGG-3′, Invitrogen, Thermo Fisher). For all the studied miRs, the sequence of the universal primer was 5′-GAATCGAGCACCAGTTACGC-3′. All the RT-qPCRs were conducted using the CFX96 Real-Time PCR Detection System combined with CFX Manager software (Bio-Rad Laboratories).

Western blot. Due to the identical culturing and methodological arrangements, the same protein lysates and Western blot protocol were used as we previously described (8). Briefly, 10 µg of protein was loaded on 4%–20% Criterion TGX Stain-Free protein gels (No. 5678094, Bio-Rad Laboratories) followed by separation using SDS-PAGE. Stain-free technology was used to control loading and for data normalization to the total protein content. After blocking, the

primary antibodies were probed overnight at 4°C. The primary antibodies purchased from Cell Signaling Technology (Danvers, MA, USA) and their dilutions used were as follows: p-C/EBPβ^{Thr235} (#3084, 1:1000), p-Iκβ/α$^{Ser32/36}$ (#9246, 1:1000), p-IKKα/β$^{Ser176/180}$ (#2697, 1:1000), p-NF-κB^{Ser536} (#3033, 1:1000), p-STAT3^{Tyr705} (#9145, 1:1000) and STAT3 (#9139, 1:1000). The CCL2/MCP1 (NBP1-07034, 1:1000) was purchased from Novus Biologicals (Littleton, CO, USA) and MYH1E (MF 20, concentrate, 1:3000) from Developmental Studies Hybridoma Bank (Iowa City, IA, USA). The horseradish peroxidase-conjugated secondary IgG anti-mouse (1:30 000) and anti-rabbit (1:10 000) antibodies were purchased from Jackson ImmunoResearch Laboratories (West Grove, PA, USA). Enhanced chemiluminescence (SuperSignal west femto maximum sensitivity substrate; Pierce Biotechnology, Rockford, IL, USA) and ChemiDoc MP device (Bio-Rad Laboratories) were used for protein visualization.

Bioinformatic analyses. The mRNA-seq data analysis steps from the initial quality check to differential expression analysis were conducted using Chipster software (https://chipster.csc.fi/) (27), while sRNA-seq sequence processing was conducted using CLC Genomics Workbench version 22 software (Qiagen), and further data analyses with edgeR. In more detail, for the mRNA data processing, the read quality was first analyzed using multiQC for many FASTQ files. The quality control results show Phred scores ranging from over 30 in the beginning of the sequences to about 23 at the base 300. The mean per-sequence Phred score was 27.9. and the mean sequence length was 155 bases. Next, the reads were aligned to the selected genome using STAR for single-ended reads. To count the number of aligned reads per gene, HTSeq tool was used. The average number of reads per sample was 346 191, resulting on average of 255 387 reads being unambiguously mapped to the genes. The maximum read sequence number per run using the Ion Torrent PGM chips is approximately 400 000 – 560 000 per sample for 20 samples. Our average was 346 191 reads per sample showing adequate technical success. About 23% of the reads were discarded because they could be aligned to more than one region. The total number of unique genes identified was 15 273 and this data was further analyzed to determine the differentially expressed genes (DEGs) using edgeR. From this step onwards, the data were analyzed using following software's: Gene Set Enrichment Analysis (GSEA, https://www.gsea-msigdb.org/gsea/index.jsp), Ingenuity Pathway Analysis (IPA, Qiagen, https://digitalinsights.qiagen.com) and ShinyGO (28) (http://bioinformatics.sdstate.edu/go/). The

GSEA is frequently used in exercise studies due to its low bias and ability to reveal changes in expression of a large set of genes even when the average change of gene expression is 20% or even lower (29, 30), which typically is the case with exercise (31, 32). The GSEA was conducted using fgsea R-package as previously described (33). The GSEA analysis included genes with at least 4 reads in the comparisons. When using ShinyGO, only DEGs (FDR < 0.05) from pool of the stimulated vs. pool of the non-stimulated comparison (EPS main effect) as well as all the genes as background (including more than 4 reads per sample) were input to analysis. For miRNAs, on average 2.39 M reads per sample were processed, adapter sequences were trimmed and 9-40 bp long sequences were selected for the analyses. Reads (1.1 M – 2.3 M per sample after trimming) were annotated against miRbase-Release_v22 (*Mus musculus*), allowing length-based isomiRs, 2 additional/missing upstream and downstream bases and mismatches. In the case of sRNA-seq, miRNAs with very low expression (less than 5 samples with at least 2 counts) were filtered out. The miRNA counts were normalized by trimmed mean of M values (TMM) method (34) using edgeR-package (35). Overall, we detected 163 miRNAs from the EVs and of these, the top 50 miRNAs with the highest normalized expression were chosen for further analyses unless otherwise stated.

Statistical analyses. The statistical significance was set at Benjamini-Hochberg corrected false discovery rate (FDR) < 0.05 for multiple testing and fold change (FC) > | 1.2 | to discover DEGs. These DEG´s were directed for the pathway/enrichment analyses using IPA (all comparisons) and ShinyGO (EPS main effect). For GSEA, all expressed mRNAs (which had at least 4 reads in total) were ranked in all the comparisons and used for the further GSEA. For the statistical evaluation of the main and interaction effects in sRNA-seq, RT-qPCR (cell lysates) and Western blot, the two-way multivariate analysis of variance (two-way MANOVA) was used, while the group comparisons were performed using multivariate Tukey's test (IBM SPSS Statistics, version 26 for Windows, SPSS Chicago, IL, USA). PERMANOVA analysis of normalized miRNA counts was carried out using *vegan* R-package (36) and all the 163 miRNAs. The miRNA RT-qPCR results (group comparisons as well as EL-EPS and glucose effects) were analyzed using Mann Whitney *U*-test (IBM SPSS Statistics). The extreme outliers from all the RT-qPCR analyses were removed based on Grubbs´ test (https://www.graphpad.com). GraphPad Prism software (v10.0.2) was used to prepare the bar graphs. The VIsualization and Integration

279 of Metabolomics Experiments (VIIME) software (https://viime.org) was used to generate the
280 principal component analysis (PCA) score plot and the heat maps (37). Some of the plots were
281 generated using the ggplot2 package (38) in the R programming language (version 4.3.1). The
282 data is presented as means ± SEM unless otherwise stated. The level of statistical significance
283 was set at $P < 0.05$ when FDR was not used.

RESULTS

Higher glucose availability augmented gene expression responses after EL-EPS

The effects of EL-EPS and media glucose content on the C2C12 myotube transcriptome were analyzed after the 24-hour EL-EPS by mRNA-seq. We observed eight and 66 DEGs in LG and HG conditions after EL-EPS, respectively (Figure 2A). A comparison of the combined LG and HG groups with and without EL-EPS (EPS effect) resulted in 65 DEGs (Figure 2A). Altogether, six DEGs (*Cxcl1*, *Cxcl5*, *Myh2*, *Tceal7*, *Csrp3* and *Ier3*) were shared between these three comparisons (Figure 2A). The principal component analysis (PCA) of the DEGs showed that the stimulated and non-stimulated groups were clearly separated independent of the glucose availability (Figure 2B). The heat map clustering of the DEGs show that all eight DEGs observed under LG condition were upregulated, while HG condition (50 up- and 16 downregulated DEGs) and EPS effect (50 up- and 15 downregulated DEGs) resulted in substantially more up- than downregulated DEGs (Figure 2C-E).

To complement the mRNA-seq results, we analyzed the expression of a few of the most up- and downregulated genes by RT-qPCR. Concordantly with the mRNA-seq results, in comparison to non-stimulated myotubes, the expression of *Cxcl1*, *Cxcl5* and *Tceal7* were higher (EPS main effects, $P < 0.05$) and *Scml4* was lower (EPS main effect, $P = 0.057$) in the EL-EPS-stimulated myotubes (Figure 3A-D).

Pathways related to myotube contractibility and inflammatory responses were upregulated in response to EL-EPS independent of the glucose availability

To understand the pathways to which the identified DEGs belong, we conducted bioinformatic analyses using Gene Set Enrichment Analysis (GSEA) and Ingenuity Pathway Analysis (IPA). The GSEA analysis was performed by using the Gene Ontology Biological Processes (GOPB) database (Figure 4A-B) and for completeness, this analysis was also run with Kyoto Encyclopedia of Genes and Genomes (KEGG) and REACTOME databases (Figure S1 and Table S1). Regardless of the database used, we found that the enriched pathways after EL-EPS were mainly related to muscle architecture and contractile ability as well as cytokine and

311 inflammatory responses, independent of the media glucose availability (Figure 4A-B, Figure S1
312 and Table S1). The IPA analyses showed that the DEGs with molecular and cellular functions
313 related to growth, proliferation, development, movement, assembly, and organization were
314 upregulated by EL-EPS as were intercellular signaling and interaction pathways. To complement
315 GSEA and IPA analyses, ShinyGo analysis was conducted. By using this approach, we observed
316 that EL-EPS induced 180 enriched GOPBs, 9 KEGG, 4 REACTOME, 9 Gene Ontology
317 Molecular Functions and 13 Gene Ontology Cellular Component (FDR < 0.05, Table S2). With
318 ShinyGO, many processes were similar as with GSEA and IPA in response to EL-EPS, including
319 processes related to contractility and inflammatory response (Figure 4, Figure S1, Table S1 and
320 Table S2).

321 Notably, we aimed to compare our previous metabolomics (8) and the present transcriptomics
322 data to conduct trans-omic analyses using Metscape module in the Cytoscape platform
323 (https://cytoscape.org). Our ^{1}H-NMR metabolomics revealed significant changes in energy
324 metabolism related intermediates (8), while only a small number of changes in metabolic DEGs
325 were observed in the present study. Given the paucity of metabolic transcriptional changes,
326 MetScape analysis did not reveal interactions between the omics.

327 It is interesting to note that there were very few alterations in metabolic pathways identified in
328 any of the datasets. Using the KEGG database, we observed an increase in the normalized
329 enrichment score (NES) in oxidative phosphorylation in response to myotube contractions in LG
330 conditions along with an increase in both the pentose phosphate pathway (PPP) and fructose &
331 mannose metabolism in stimulated versus non-stimulated conditions (EPS vs. CTRL, Figure S1
332 and Table S1). The REACTOME database revealed an increase in tricarboxylic acid cycle and
333 respiratory electron transport in response to myotube contractions in LG conditions (Figure S1
334 and Table S1).

335 To elucidate whether the activities of some of the pathways suggested by the bioinformatic
336 analyses were affected at the protein level, we analyzed the myosin heavy chain 1 isoform (MF
337 20) content and cytokine/inflammatory pathways (CCL2, p-C/EBPβ^{Thr235} p-IKKα/β$^{Ser176/180}$, p-
338 Iκβ/α$^{Ser32/36}$, p-NF-κB^{Ser536}, p-STAT3^{Tyr705} and STAT3) from the C2C12 myotubes after EL-EPS.
339 Of these, when compared to the respective controls, the phosphorylation of NF-κB^{Ser536} was

greater in response to EL-EPS and media glucose content (EPS main effect, $P < 0.05$ and glucose main effect, $P < 0.01$, respectively, Figure 5A). The phosphorylation level or the content of CCL2, MF 20, $STAT3^{Tyr705}$ and total STAT3 remained unaffected (Figure 5B-E), whereas p-$C/EBP\beta^{Thr235}$, p-$IKK\alpha/\beta^{Ser176/180}$ and p-$I\kappa\beta/\alpha^{Ser32/36}$ were undetected.

Although media glucose content had greater effects on EV miRNAs than EL-EPS, packing of exercise-responsive miR-1-3p into EVs was greater after stimulation

To elucidate whether miRNA-release occurs in cultured myotubes in response to EL-EPS, we collected the cell culture media, extracted the EVs and analyzed the representative samples using nanoparticle tracking analysis and electron microscopy. Based on the nanoparticle tracking analysis of the representative samples, the EV number appears to be greater in the HG media and lower in LG media of the stimulated myotubes in comparison to non-stimulated myotubes, while electron microscopy showed that the extracted EVs were of the expected size (~100 nm) in all conditions (Figure S2).

Next, we analyzed EV samples using sRNA-seq. Our sRNA-seq data showed that the C2C12 myotubes release EVs with similar miRNA content as previously reported for *in vivo* skeletal muscle (13), including miR-206-3p, miR-1-3p and miR-133a-3p (Figure 6A, Table S2). Further data analysis of the top 50 most abundant miRNAs showed that media glucose availability had a greater effect on EV miRNA content than EL-EPS. In more detail, based on the heat map clustering, eight miRNAs were affected by media glucose content and none by the EL-EPS. More specifically, the content of miR-196a-5p, let-7f-5p and miR-26a-5p in EVs were higher in HG conditions, while miR-378c, miR-378a-3p, miR-322-5p, miR-140-3p and miR-19b-3p were higher in LG conditions (HG main effect, $P < 0.05$, Figure 6B). However, when we further analyzed all the 163 miRNAs using PERMANOVA analysis, we found no differences between any of the groups. In addition to sRNA-seq, we used RT-qPCR to analyze the expression of a few best-known exercise-responsive miRNAs from the EVs. Based on these analyses, we demonstrate that similar to *in vivo* exercise, myotube contractions increased the packing of specific miRNAs to the released EVs. More specifically, when compared to the respective controls, the expression of miR-1-3p was greater in response to EL-EPS (EPS effect, $P < 0.05$), while miR-206-3p expression tended to be greater (EPS effect, $P = 0.074$) (Figure 6C-D).

369 Numerically miR-133a-3p also increased by several fold, but due to high inter-sample variation,
370 this result was non-significant (EPS effect, P = 0.242) (Figure 6E).

DISCUSSION

The number of *in vitro* studies examining transcriptional changes after EL-EPS has increased rapidly in recent years (10, 39–45), but, to our knowledge, studies investigating the interaction between nutritional availability and the exercise responses are lacking. In the present study, we demonstrate that the contraction-induced changes in the C2C12 myotube transcriptome including reorganization of contractile units and cytokine/inflammatory responses were amplified under high glucose compared to low glucose condition. This supports our previous metabolomics findings showing that higher glucose availability augmented metabolic responses in the contracting C2C12 myotubes (8). Notably, more DEGs and pathways were up- than downregulated in response to myotube contractions, which suggests that especially under high glucose condition, the repressors of transcription were overrun by the activators. Furthermore, to the best of our knowledge, this is the first study to analyze skeletal muscle cell-derived EVs and their miRNA content after EL-EPS conducted under variable nutritional conditions. We report that several miRNAs were released from the C2C12 myotube-derived EVs and show that packing of miR-1-3p into the EVs was increased in response to myotube contractions independent of the glucose availability. Our sRNA-seq findings, however, suggest that glucose availability has more prominent effects on myotube EV miRNA content than the EL-EPS.

Based on the pathway analyses, the most upregulated cellular processes after EL-EPS were related to myotube contraction and structural modifications as well as cytokine and other inflammatory responses. The myotubes do not contract immediately after EL-EPS due to the lack of adequate sarcomere architecture (46). *De novo* sarcomere assembly and reorganization of the cytoskeleton are needed for the visible contractions and thus it is reasonable that muscle filament sliding, myofibril assembly, sarcomere organization, and muscle contraction pathways were upregulated in response to EL-EPS independent of the glucose availability. We showed in agreement with previous findings (10, 47) that although the gene expression of different myosin heavy chain isoforms was upregulated in response to myotube contractions especially when more glucose was available, the protein level of at least myosin heavy chain 1 isoform remained unaltered. Previously the absence of mRNA-protein correlations has been explained by the post-

399 transcriptional mechanisms needed for the mRNA to be turned into protein as well as by broad
400 range of protein half-lives (48). The changes in myosin heavy chain isoforms may be explained
401 by the fact that the skeletal muscle cells in the culture are at variable differentiation stages.
402 Indeed, differentiation of the C2C12 myoblasts into myotubes has been shown to increase the
403 expression of variable myosin heavy chain isoforms (49), while *Tceal7*, a gene previously related
404 to improved muscle cell differentiation after muscle damage (50) was also upregulated after EL-
405 EPS independent of the glucose availability. Moreover, EL-EPS itself may also promote
406 differentiation and maturation of the myoblasts into myotubes (51, 52). Overall, our results
407 suggest that repeated contractions promoted remodeling of the myotube architecture to promote
408 contractility and possibly differentiation of the cells, especially with high glucose availability.

409 Similar to *in vivo* exercise (53), cytokine and other inflammatory pathways including response to
410 chemokine, chemokine signaling pathway, and cytokine signaling in the immune system were
411 enhanced after EL-EPS, and we found that this occurred independent of the glucose availability.
412 Concordantly with the previous EL-EPS studies (39, 41, 54, 55), the expression of the members
413 belonging to the CXC (*Cxcl1*, *Cxcl5* and *Cx3cl1*) and CC (*Ccl2* and *Ccl7*, also known as
414 monocyte chemoattractant protein (MCP)-1 and MCP-3, respectively) chemokine families were
415 upregulated after EL-EPS, especially with high glucose availability. Others have demonstrated
416 that many of the CXC and CC chemokines are released into the circulation/cell culture media in
417 response to exercise and/or muscle cell/myotube contractions (39, 54–56), probably partly via
418 β2-adrenoceptor antagonist (clenbuterol)-mediated mechanisms (10). *In vivo*, cytokine and other
419 inflammatory responses induced by acute exercise may promote the infiltration of macrophages
420 into the skeletal muscle (57). This could enhance skeletal muscle regeneration and/or
421 hypertrophy possibly via CXCL1, CX3CL1 and CCL2 (57–59). *In vitro*, the increased media
422 content of CXCL1 and CXCL5 have been reported to regulate C2C12 myoblast migration and
423 differentiation after EL-EPS (58, 60), while CCL2 release into the media in a NF-κB-dependent
424 manner may promote monocyte chemoattraction *in vitro* and possibly infiltration *in vivo* (58).
425 Supporting the potential chemokine and inflammatory signaling after EL-EPS, we observed
426 increased phosphorylation (activation) of NF-κB, which supports some (39, 58), but not all (47)
427 studies. To summarize, together our results show that EL-EPS produced similar cytokine and
428 inflammatory responses in the skeletal muscle cells as does *in vivo* exercise and that these

429 responses were augmented by higher glucose availability. These processes are important to
430 promote exercise-induced adaptations in the skeletal muscle *in vivo* (61), but this remains to be
431 demonstrated *in vitro*.

432 Besides contractility and inflammation, many metabolic processes were affected by EL-EPS. We
433 have previously reported that EL-EPS enhanced glycolysis in the myotubes based on the
434 increased lactate production and release, especially with high glucose availability (8). Here we
435 report concordantly that the expression of phosphofructokinase liver B-type (*Pfkl*) and pyruvate
436 dehydrogenase kinase 1 (*Pdk1*) increased after EL-EPS. Phosphofructokinase is the key enzyme
437 regulating glycolysis. Pyruvate dehydrogenase (PDH) promotes the conversion of pyruvate to
438 acetyl-CoA, while enhanced PDK1 activation shifts the conversion of pyruvate towards lactate
439 (62). Previously, the phosphorylated form of PDH has been reported to decrease in the C2C12
440 cells after EL-EPS (42), which could increase the activity of the PDH enzyme and promote
441 glucose oxidation in the cells, a response we previously reported after EL-EPS (8). In addition to
442 increased lactate synthesis, lactate transport mechanisms may have been enhanced in response to
443 myotube contractions. The solute carrier family 16 member 3 (*Slc16a3*, also known as MCT4)
444 was upregulated in response to EL-EPS. It belongs to the monocarboxylate cotransporter (MCT)
445 family that transport e.g., pyruvate and lactate across different membranes (63). The significance
446 of SLC16A3 in the regulation of lactate efflux might be elevated in glycolytic cells (63) and
447 indeed, the C2C12 myotubes can be considered relatively glycolytic cells (44). Together, the
448 changes we have observed both at the levels of metabolites (8) and transcription in this study
449 show that the production and probably handling of lactate were improved in the C2C12
450 myotubes in response to EL-EPS. These observations are in accordance with human data on
451 lactate metabolism in response to exercise (64).

452 In addition to glycolysis, pentose phosphate pathway (PPP), a parallel metabolic pathway to
453 glycolysis, was among the overrepresented processes in response to myotube contractions. In
454 accordance, others have previously observed contraction-induced activation of PPP in the C2C12
455 myotubes after short-term high-frequency EL-EPS (42). They suggested that PPP activation
456 might occur partly via reactive oxygen species (ROS) as well as Akt, extracellular regulated

457 kinase (ERK) and c-Jun N-terminal kinase (JNK) signaling (42). Notably, we have also reported
458 increased JNK phosphorylation after EL-EPS accompanied with increased glycolytic metabolism
459 (8). Parallel to glycolysis, activation of PPP pathway after EL-EPS may be an adaptive response
460 to myotube contractions (42) to support the synthesis of nucleotides, certain aromatic amino
461 acids and lipids needed for e.g., hypertrophy and membrane recovery (65). Related to PPP
462 activation and ROS, we observed contraction-induced upregulation in the expression of
463 superoxide dismutase 3, extracellular (*Sod3*) as well as another possibly exercise-responsive (66)
464 redox enzyme participating in antioxidant defense, glutaredoxin (*Glrx*). In accordance, ROS has
465 been suggested to regulate transcription of antioxidant enzymes including SOD and glutathione
466 peroxidase-1 (GPX1) after *in vivo* exercise (67). *In vitro*, others have shown that adequate
467 protection against excessive ROS effects seems to be important to maintain myotube contractility
468 (68) and mitochondrial function (69) during EL-EPS. Thus, future studies are recommended to
469 examine how different EL-EPS protocols affect distinct pathways, including PPP and ROS, and
470 what is their physiological significance.

471 The circulating miRNAs respond rapidly to exercise stimulus (70), thus making them an
472 interesting group of potential exerkines to study not only *in vivo* but also *in vitro*. To date,
473 miRNA studies have focused on *in vivo* exercise (for review, see(13, 17)) showing that, for
474 example, miR-1, miR-21, miR-133, miR-155 and miR-206 could act as biomarkers of changes in
475 exercise capacity (71). Additionally, human primary myotubes have also been previously shown
476 to release miR-1 containing EVs in response to EL-EPS (72). Concordantly with these studies,
477 we demonstrate that miR-1-3p as well as potentially miR-206-3p and miR-133a-3p, were
478 increased in the EVs in response to myotube contractions independent of the media glucose
479 availability thus suggesting these could act as potential exerkines. Among other processes, EV-
480 derived miRNAs have been shown to promote myoblast differentiation (73). More specifically,
481 in the C2C12 cells miR-1 enhanced myogenesis, while miR-133a promoted proliferation (74).
482 Additionally, miR-206 has been shown to promote differentiation of the C2C12 cells (75).
483 Beyond differentiation, miR-1 regulates e.g., mitochondrial metabolism (76, 77), while miR-
484 133a may be an important mediator of exercise-induced adaptations in the skeletal muscle (78).
485 miR-206 is involved in processes related, but not limited to, skeletal muscle development,
486 growth/adaptation and regeneration (79). Although *in vivo* studies have demonstrated that the

number of circulating EVs increases during exercise (14), this might not be the case *in vitro* (80). We observed that the EV number was possibly increased in high, but not in low glucose condition. This suggests that myotube contractions increased the abundance of the miRNAs, but not necessarily the number of EVs. Others have shown that short-term low-frequency EL-EPS had no effects on EV size distribution or protein markers (80). Yet, as in the present study the EV number was investigated only from a representative sample and not individual samples, this needs to be verified in future studies.

Although both sRNA-seq and RT-qPCR identified similar miRNAs that have been linked to *in vivo* skeletal muscle and exercise (13, 16), our results were not fully compatible between the methods. Based on the sRNA-seq, media glucose content had greater effects on the EV-carried miRNAs than EL-EPS, while RT-qPCR showed contraction-induced increase in the miR-1-3p content, which was not confirmed by sRNA-seq. These observations are likely explained by methodological differences. Most importantly, normalization of the sRNA-seq and RT-qPCR results differ from each other (i.e., trimmed mean of M values (34) vs. spike-in cel-miR-39-3p, respectively). Furthermore, it has been previously shown that when comparing RT-qPCR to RNA-seq, 15–20% of protein coding genes were considered as non-concordant, and these genes were typically lower expressed and shorter (81). Since our study focused on sRNAs that are expressed at relatively low abundancy in cell media EVs, it is likely that these factors, together with the normalization, explain the observed difference between sRNA and RT-qPCR results. Finally, most of the sRNAs identified by sRNA-seq were other than miRNAs, while RT-qPCR approach used focuses more selectively on miRNAs. To summarize the miRNA results, in agreement with the existing literature, we show that miR-1-3p content in the EVs was greater in response to EL-EPS, but more research is needed to gain a comprehensive view of miRNA/sRNA packing and EV release in response to myotube and muscle contractions.

In vivo, greater disturbances in the skeletal muscle metabolism are thought to augment exercise-induced adaptations (82). The type, intensity and duration of exercise can increase the metabolic load in the skeletal muscle and possibly lead to greater adaptations, while also nutritional strategies can be used. Indeed, carbohydrate restriction and training under low carbohydrate

availability and glycogen-depleted state have been shown to enhance some of the metabolic adaptations to endurance exercise, such as mitochondrial biogenesis (11). Interestingly, we report here that myotube contractions induced greater responses in the gene expression as well as previously in the metabolites (8) under HG condition. The reason for these responses may be related to the viability of the cells. Our metabolomics studies showed that glucose was almost completely depleted from the media and cells under low glucose condition (8), which may limit the metabolism of these glycolytic C2C12 cells relying heavily on carbohydrate metabolism. However, other processes, such as miRNA packing and previously reported exerkine secretion and fatty acid oxidation (8) were less affected by the media glucose content. To summarize, our current and previous (8) omics-analyses suggest that lower glucose availability may compromise contraction-induced effects on the myotubes and result in smaller metabolic perturbations. Notably, based on the analyzed markers, no unique responses or pathways were observed in low glucose condition in response to myotube contractions. Moreover, similar to metabolomics (8), the observed contraction-induced changes at the level of transcription remained either unaltered or less affected when less glucose was available. More research is warranted to study the effects of nutritional availability on myotube metabolism in response to different types of EL-EPS, e.g., stimulation with higher frequency and/or voltage and with shorter durations. It would be important to better understand whether the glucose availability *per se* influences the contraction-induced responses in the myotubes or can the results be explained by some other mechanisms that occur due to culturing in high or low glucose containing media. Finally, as higher media glucose content augmented omics responses of the C2C12 myotubes after EL-EPS based on our present and previous (8) experiments, future studies are recommended to consider and report media composition carefully.

LIMITATIONS OF THE STUDY

Although the use of EL-EPS and myotubes as an *in vitro* exercise model is well established and we report many similar responses in the myotube gene expression and EV miRNA content as has been reported after *in vivo* exercise, this approach does not fully represent *in vivo* exercising human muscle due to the murine origin of the C2C12 cells and the lack of other cell types, such as vascular cells. Moreover, myotube cultures always contain myoblasts, but EL-EPS has been

544 mainly suggested to target myotubes. As an example, interleukin 6, a well-known exerkine, is
545 released mainly from the differentiated and contracting myotubes (83). Thus, caution is needed
546 when interpreting the results in relation to *in vivo* findings, especially in human studies. In the
547 future, more time course studies are needed to better examine rapid and transient contraction-
548 induced changes, such as cytokine bursts (84) and EV/miRNA responses (85) or delayed
549 metabolic effects, such as myotube hypertrophy (86).

550 From the methodological point of view, EVs are complicated transport vehicles to work with due
551 to their low abundance in the cell culture media. For example, of the small RNAs analyzed using
552 sRNA-seq, less than 1% were miRNAs. The majority of the RNAs found in EVs were e.g.,
553 transfer RNAs and ribosomal RNAs. Thus, the future studies are recommended to analyze not
554 only these less well-known RNAs using e.g., PANDORA-seq (87), but also to pool media from
555 multiple wells for one EV extraction to obtain adequate amount of starting material for the
556 downstream analyses. Overall, despite the small sample amount, the EV miRNA results
557 presented in this study, especially related to sRNA-seq and nanoparticle tracking analyses, are
558 paving the way for more in-depth analysis in the future.

559 **CONCLUSION**

560 In conclusion, we show that the transcriptional responses of the C2C12 myotubes to EL-EPS
561 were augmented by higher media glucose availability. Based on the pathway analyses, cellular
562 processes including especially contractility and cytokine/inflammatory response were
563 upregulated in response to myotube contractions independent of the media glucose content.
564 However, only modest changes in these pathways were seen at the level of translation/protein
565 phosphorylation. In accordance with the previous literature, we also show that EL-EPS increased
566 myotube release and packing of miR-1-3p into the EVs, showing that as *in vivo* studies have
567 suggested, this indeed is a potential exerkine. Yet, further studies are warranted to better
568 understand how muscle contractions and different nutritional states regulate miRNA and EV
569 responses. Together our results hopefully enable the development of more realistic *in vitro*
570 exercise models.

DATA AVAILABILITY

The source data from mRNA (Table S4) and sRNA (Table S5) sequencing analyses (read counts) are available at:

Table S4:

URL: https://figshare.com/s/ea20ef3da4f131b0a0d3

DOI: https://doi.org10.6084/m9.figshare.23931369

Table S5:

URL: https://figshare.com/s/4a1f3658fff4dbb8be6a

DOI: https://doi.org10.6084/m9.figshare.23931375

SUPPLEMENTAL MATERIAL

The Supplemental Material is available at:

Figure S1:

URL: https://figshare.com/s/b82719d36229d6a241d0

DOI: https://doi.org10.6084/m9.figshare.23918376

Figure S2:

URL: https://figshare.com/s/72e6eade83a688d7012f

DOI: https://doi.org10.6084/m9.figshare.23918415

Table S1:

URL: https://figshare.com/s/b481cf99bc5dfe1f283d

DOI: https://doi.org10.6084/m9.figshare.23918385

Table S2:

URL: https://figshare.com/s/3105dca76c68d1563ca7

DOI: https://doi.org10.6084/m9.figshare.24476524

Table S3:

URL: https://figshare.com/s/0e6f57c723e13de89b27

DOI: https://doi.org10.6084/m9.figshare.23918475

ACKNOWLEDGEMENTS

We acknowledge the services of university of Helsinki: EV core in FIMM Technology Centre supported by HiLIFE and Biocenter Finland for performing nanoparticle tracking analysis and electron microscopy work and Electron Microscopy Unit of the Institute of Biotechnology for providing the facilities. We appreciate the help received from Emeritus Professor Urho Kujala and Associate Professor Eija Laakkonen for the experimental procedures and reagents. We thank Elina Virtanen for the help in sequencing.

GRANTS

The Academy of Finland (now Research Council of Finland) (Grant No. 332946 to S.K., 323063 to M.T., 275922 to J.J.H, and 308042 to S.P.), Emil Aaltonen Foundation (to J.H.L-K) and the Finnish Cultural Foundation (to J.H.L-K.) funded this work. T. M. O. was supported by grants from National Institutes of Health, National Institute of Arthritis and Musculoskeletal and Skin Diseases (P01AG039355 and P30AR072581) and the Additional Ventures, Single Ventricle Research Fund. The Research Council of Finland funded profiling of the University of Jyväskylä (Profi5 301824 funding: Physical ACTivity and health during the human life-Span 2, PACTS2) and the University of Oulu (Profi6 336449 funding: Fibrobesity – Preventing fibrosis related to obesity) also supported the study.

AUTHOR CONTRIBUTIONS

J.H.L-K., J.J.H. and S.P. conceived and designed research, J.H.L-K., performed experiments, J.H.L-K., S.K., T-M.K., T.M.O. and M.T. analyzed data, J.H.L-K., S.K. T.M.O., J.J.H. and S.P. interpreted results of experiments, J.H.L-K. and T.M.O. prepared figures, J.H.L-K. drafted manuscript, S.K., T-M.K, T.M.O., M.T., J.J.H., and S.P. edited and revised manuscript, all authors approved final version of manuscript.

DISCLOSURES

No conflicts of interest, financial or otherwise, are declared by the authors.

622

623 **REFERENCES**

624 1. **Pedersen BK**, **Saltin B**. Exercise as medicine - evidence for prescribing exercise as
625 therapy in 26 different chronic diseases. *Scand J Med Sci Sports* 25: 1–72, 2015.

626 2. **Severinsen MCK**, **Pedersen BK**. Muscle–Organ Crosstalk: The Emerging Roles
627 of Myokines. *Endocr Rev* 41: 594–609, 2020.

628 3. **Chow LS**, **Gerszten RE**, **Taylor JM**, **Pedersen BK**, **van Praag H**, **Trappe S**,
629 **Febbraio MA**, **Galis ZS**, **Gao Y**, **Haus JM**, **Lanza IR**, **Lavie CJ**, **Lee C-H**, **Lucia**
630 **A**, **Moro C**, **Pandey A**, **Robbins JM**, **Stanford KI**, **Thackray AE**, **Villeda S**,
631 **Watt MJ**, **Xia A**, **Zierath JR**, **Goodpaster BH**, **Snyder MP**. Exerkines in health,
632 resilience and disease. *Nat Rev Endocrinol* 18: 273–289, 2022.

633 4. **Safdar A**, **Saleem A**, **Tarnopolsky MA**. The potential of endurance exercise-
634 derived exosomes to treat metabolic diseases. *Nat Rev Endocrinol* 12: 504, 2016.

635 5. **Carter S**, **Solomon TPJ**. In vitro experimental models for examining the skeletal
636 muscle cell biology of exercise: the possibilities, challenges and future
637 developments. *Pflügers Archiv-European Journal of Physiology* 471: 413–429,
638 2019.

639 6. **Nikolić N**, **Görgens SW**, **Thoresen GH**, **Aas V**, **Eckel J**, **Eckardt K**. Electrical
640 pulse stimulation of cultured skeletal muscle cells as a model for in vitro exercise -
641 possibilities and limitations. *Acta Physiologica* 220: 310–331, 2017.

642 7. **Lautaoja JH**, **Turner DC**, **Sharples AP**, **Kivelä R**, **Pekkala S**, **Hulmi JJ**, **Ylä-**
643 **Outinen L**. Mimicking exercise in vitro: effects of myotube contractions and
644 mechanical stretch on omics. *American Journal of Physiology-Cell Physiology* 324:
645 C886–C892, 2023.

8. **Lautaoja JH**, **O'Connell TM**, **Mäntyselkä S**, **Peräkylä J**, **Kainulainen H**, **Pekkala S**, **Permi P**, **Hulmi JJ**. Higher glucose availability augments the metabolic responses of the C2C12 myotubes to exercise-like electrical pulse stimulation. *American Journal of Physiology-Endocrinology and Metabolism* 321: E229–E245, 2021.

9. **MacDonald TL**, **Pattamaprapanont P**, **Pathak P**, **Fernandez N**, **Freitas EC**, **Hafida S**, **Mitri J**, **Britton SL**, **Koch LG**, **Lessard SJ**. Hyperglycaemia is associated with impaired muscle signalling and aerobic adaptation to exercise. *Nat Metab* 2: 902–917, 2020.

10. **Fukushima T**, **Takata M**, **Kato A**, **Uchida T**, **Nikawa T**, **Sakakibara I**. Transcriptome Analyses of In Vitro Exercise Models by Clenbuterol Supplementation or Electrical Pulse Stimulation. *Applied Sciences* 11: 10436, 2021.

11. **Hawley JA**. Sending the Signal: Muscle Glycogen Availability as a Regulator of Training Adaptation. In: *Spiegelman B. (eds) Hormones, Metabolism and the Benefits of Exercise. Research and Perspectives in Endocrine Interactions.* Springer, Cham, 2017, p. 43–55.

12. **Wang H**, **Wang B**. Extracellular vesicle microRNAs mediate skeletal muscle myogenesis and disease. *Biomed Rep* 5: 296–300, 2016.

13. **Vechetti IJ**, **Valentino T**, **Mobley CB**, **McCarthy JJ**. The role of extracellular vesicles in skeletal muscle and systematic adaptation to exercise. *J Physiol* 599: 845–861, 2021.

14. **Whitham M**, **Parker BL**, **Friedrichsen M**, **Hingst JR**, **Hjorth M**, **Hughes WE**, **Egan CL**, **Cron L**, **Watt KI**, **Kuchel RP**. Extracellular Vesicles Provide a Means for Tissue Crosstalk during Exercise. *Cell Metab* 27: 237–251, 2018.

15. **Karvinen S**, **Korhonen T**, **Sievänen T**, **Karppinen JE**, **Juppi H**, **Jakoaho V**, **Kujala UM**, **Laukkanen JA**, **Lehti M**, **Laakkonen EK**. Extracellular vesicles and high-density lipoproteins: Exercise and oestrogen-responsive small RNA carriers. *J Extracell Vesicles* 12: 12308, 2023.

16. **Siqueira IR**, **Palazzo RP**, **Cechinel LR**. Circulating extracellular vesicles delivering beneficial cargo as key players in exercise effects. *Free Radic Biol Med* 172: 273–285, 2021.

17. **Nederveen JP**, **Warnier G**, **Di Carlo A**, **Nilsson MI**, **Tarnopolsky MA**. Extracellular Vesicles and Exosomes: Insights From Exercise Science. *Front Physiol* 11: 1757, 2021.

18. **van Niel G**, **D'Angelo G**, **Raposo G**. Shedding light on the cell biology of extracellular vesicles. *Nat Rev Mol Cell Biol* 19: 213, 2018.

19. **Lautaoja JH**, **Pekkala S**, **Pasternack A**, **Laitinen M**, **Ritvos O**, **Hulmi JJ**. Differentiation of Murine C2C12 Myoblasts Strongly Reduces the Effects of Myostatin on Intracellular Signaling. *Biomolecules* 10: 695, 2020.

20. **Furuichi Y**, **Manabe Y**, **Takagi M**, **Aoki M**, **Fujii NL**. Evidence for acute contraction-induced myokine secretion by C2C12 myotubes. *PLoS One* 13: e0206146, 2018.

21. **Simonsen JB**. What Are We Looking At? Extracellular Vesicles, Lipoproteins, or Both? *Circ Res* 121: 920–922, 2017.

22. **Evtushenko EG**, **Bagrov D v.**, **Lazarev VN**, **Livshits MA**, **Khomyakova E**. Adsorption of extracellular vesicles onto the tube walls during storage in solution. *PLoS One* 15: e0243738, 2020.

23. **Karvinen S**, **Sievänen T**, **Karppinen JE**, **Hautasaari P**, **Bart G**, **Samoylenko A**, **Vainio SJ**, **Ahtiainen JP**, **Laakkonen EK**, **Kujala UM**. MicroRNAs in extracellular vesicles in sweat change in response to endurance exercise. *Front Physiol* 11: 676, 2020.

24. **Puhka M**, **Nordberg ME**, **Valkonen S**, **Rannikko A**, **Kallioniemi O**, **Siljander P**, **Af Hällström TM**. KeepEX, a simple dilution protocol for improving extracellular vesicle yields from urine. *European Journal of Pharmaceutical Sciences* 98: 30–39, 2017.

25. **Driuchina A**, **Hintikka J**, **Lehtonen M**, **Keski-Rahkonen P**, **O'Connell T**, **Juvonen R**, **Kuula J**, **Hakkarainen A**, **Laukkanen JA**, **Mäkinen E**, **Lensu S**, **Pietiläinen KH**, **Pekkala S**. Identification of Gut Microbial Lysine and Histidine Degradation and CYP-Dependent Metabolites as Biomarkers of Fatty Liver Disease. *mBio* 14, 2023.

26. **Lautaoja JH**, **Lalowski M**, **Nissinen TA**, **Hentilä J**, **Shi Y**, **Ritvos O**, **Cheng S**, **Hulmi JJ**. Muscle and serum metabolomes are dysregulated in colon-26 tumor-bearing mice despite amelioration of cachexia with activin receptor type 2B ligand blockade. *American Journal of Physiology-Endocrinology and Metabolism* 316: E852–E865, 2019.

27. **Kallio MA**, **Tuimala JT**, **Hupponen T**, **Klemelä P**, **Gentile M**, **Scheinin I**, **Koski M**, **Käki J**, **Korpelainen EI**. Chipster: user-friendly analysis software for microarray and other high-throughput data. *BMC Genomics* 12: 507, 2011.

28. **Ge SX**, **Jung D**, **Yao R**. ShinyGO: a graphical gene-set enrichment tool for animals and plants. *Bioinformatics* 36: 2628–2629, 2020.

716 29. **Mootha VK**, **Lindgren CM**, **Eriksson K-F**, **Subramanian A**, **Sihag S**, **Lehar J**,
717 **Puigserver P**, **Carlsson E**, **Ridderstråle M**, **Laurila E**, **Houstis N**, **Daly MJ**,
718 **Patterson N**, **Mesirov JP**, **Golub TR**, **Tamayo P**, **Spiegelman B**, **Lander ES**,
719 **Hirschhorn JN**, **Altshuler D**, **Groop LC**. PGC-1α-responsive genes involved in
720 oxidative phosphorylation are coordinately downregulated in human diabetes. *Nat*
721 *Genet* 34: 267–273, 2003.

722 30. **Subramanian A**, **Tamayo P**, **Mootha VK**, **Mukherjee S**, **Ebert BL**, **Gillette MA**,
723 **Paulovich A**, **Pomeroy SL**, **Golub TR**, **Lander ES**, **Mesirov JP**. Gene set
724 enrichment analysis: A knowledge-based approach for interpreting genome-wide
725 expression profiles. *Proceedings of the National Academy of Sciences* 102: 15545–
726 15550, 2005.

727 31. **Kainulainen H**, **Papaioannou KG**, **Silvennoinen M**, **Autio R**, **Saarela J**,
728 **Oliveira BM**, **Nyqvist M**, **Pasternack A**, **AC't Hoen P**, **Kujala UM**.
729 Myostatin/activin blocking combined with exercise reconditions skeletal muscle
730 expression profile of mdx mice. *Mol Cell Endocrinol* 399: 131–142, 2015.

731 32. **Amar D**, **Lindholm ME**, **Norrbom J**, **Wheeler MT**, **Rivas MA**, **Ashley EA**.
732 Time trajectories in the transcriptomic response to exercise - a meta-analysis
733 [Online]. *Nat Commun* 12: 3471, 2021. http://www.nature.com/articles/s41467-
734 021-23579-x.

735 33. **Graber TG**, **Maroto R**, **Thompson J**, **Widen S**, **Man Z**, **Pajski ML**, **Rasmussen**
736 **BB**. Skeletal muscle transcriptome alterations related to physical function decline in
737 older mice. .

738 34. **Robinson MD**, **Oshlack A**. A scaling normalization method for differential
739 expression analysis of RNA-seq data. *Genome Biol* 11: R25, 2010.

35. **Robinson MD**, **McCarthy DJ**, **Smyth GK**. edgeR: a Bioconductor package for differential expression analysis of digital gene expression data. *Bioinformatics* 26: 139–140, 2010.

36. **Oksanen J**, **Simpson GL**, **Blanchet FG**, **Kindt R**, **Legendre P**, **Minchin PR**, **O'Hara RB**, **Solymos P**, **Stevens MHH**, **Szoecs E**, **Wagner H**, **Barbour M**, **Bedward M**, **Bolker B**, **Daniel Borcard D**, **Carvalho G**, **Michael Chirico M**, **De Caceres M**, **Sebastien Durand S**, **Antoniazi Evangelista HB**, **FitzJohn R**, **Friendly M**, **Furneaux B**, **Hannigan G**, **Hill MO**, **Lahti L**, **McGlinn D**, **Ouellette M-H**, **Ribeiro Cunha E**, **Smith T**, **Stier A**, **Ter Braak CJF**, **Weedon J**. vegan: Community Ecology Package [Online]. 2022. https://CRAN.R-project.org/package=vegan [9 Jun. 2023].

37. **Choudhury R**, **Beezley J**, **Davis B**, **Tomeck J**, **Gratzl S**, **Golzarri-Arroyo L**, **Wan J**, **Raftery D**, **Baumes J**, **O'Connell TM**. Viime: Visualization and Integration of Metabolomics Experiments. *J Open Source Softw* 5: 2410, 2020.

38. **Wickham H**. ggplot2: Elegant Graphics for Data Analysis [Online]. 3rd ed. Springer-Verlag New York. https://ggplot2.tidyverse.org [18 Jul. 2023].

39. **Scheler M**, **Irmler M**, **Lehr S**, **Hartwig S**, **Staiger H**, **Al-Hasani H**, **Beckers J**, **Hrabé de Angelis M**, **Häring H-U**, **Weigert C**. Cytokine response of primary human myotubes in an in vitro exercise model. *American Journal of Physiology-Cell Physiology* 305: C877–C886, 2013.

40. **Pourteymour S**, **Eckardt K**, **Holen T**, **Langleite T**, **Lee S**, **Jensen J**, **Birkeland KI**, **Drevon CA**, **Hjorth M**. Global mRNA sequencing of human skeletal muscle: Search for novel exercise-regulated myokines. *Mol Metab* 6: 352–365, 2017.

763 41. **Sidorenko S**, **Klimanova E**, **Milovanova K**, **Lopina OD**, **Kapilevich L v**,
764 **Chibalin A v**, **Orlov SN**. Transcriptomic changes in C2C12 myotubes triggered by
765 electrical stimulation: Role of Ca2+i-mediated and Ca2+i-independent signaling
766 and elevated [Na+]i/[K+]i ratio. *Cell Calcium* 76: 72–86, 2018.

767 42. **Hoshino D**, **Kawata K**, **Kunida K**, **Hatano A**, **Yugi K**, **Wada T**, **Fujii M**, **Sano**
768 **T**, **Ito Y**, **Furuichi Y**. Trans-omic analysis reveals ROS-dependent pentose
769 phosphate pathway activation after high-frequency electrical stimulation in C2C12
770 myotubes. *iScience* 23: 101558, 2020.

771 43. **Tamura Y**, **Kouzaki K**, **Kotani T**, **Nakazato K**. Electrically stimulated contractile
772 activity-induced transcriptomic responses and metabolic remodeling in C2C12
773 myotubes: twitch vs. tetanic contractions. *American Journal of Physiology-Cell*
774 *Physiology* 319: C1029–C1044, 2020.

775 44. **Abdelmoez AM**, **Sardón Puig L**, **Smith JAB**, **Gabriel BM**, **Savikj M**, **Dollet L**,
776 **Chibalin A v**, **Krook A**, **Zierath JR**, **Pillon NJ**. Comparative profiling of skeletal
777 muscle models reveals heterogeneity of transcriptome and metabolism. *American*
778 *Journal of Physiology-Cell Physiology* 318: C615–C626, 2020.

779 45. **Fujita H**, **Horie M**, **Shimizu K**, **Nagamori E**. Microarray profiling of gene
780 expression in C2C12 myotubes trained by electric pulse stimulation. *J Biosci*
781 *Bioeng* 132: 417–422, 2021.

782 46. **Fujita H**, **Nedachi T**, **Kanzaki M**. Accelerated de novo sarcomere assembly by
783 electric pulse stimulation in C2C12 myotubes. *Exp Cell Res* 313: 1853–1865, 2007.

784 47. **Lambernd S**, **Taube A**, **Schober A**, **Platzbecker B**, **Görgens SW**, **Schlich R**,
785 **Jeruschke K**, **Weiss J**, **Eckardt K**, **Eckel J**. Contractile activity of human skeletal

muscle cells prevents insulin resistance by inhibiting pro-inflammatory signalling pathways. *Diabetologia* 55: 1128–1139, 2012.

48. **Greenbaum D**, **Colangelo C**, **Williams K**, **Gerstein M**. Comparing protein abundance and mRNA expression levels on a genomic scale. *Genome Biol* 4: 117, 2003.

49. **Wright CR**, **Brown EL**, **Della-Gatta PA**, **Ward AC**, **Lynch GS**, **Russell AP**. G-CSF does not influence C2C12 myogenesis despite receptor expression in healthy and dystrophic skeletal muscle. *Front Physiol* 5: 170, 2014.

50. **Hulmi JJ**, **Nissinen TA**, **Räsänen M**, **Degerman J**, **Lautaoja JH**, **Hemanthakumar KA**, **Backman JT**, **Ritvos O**, **Silvennoinen M**, **Kivelä R**. Prevention of chemotherapy induced cachexia by ACVR2B ligand blocking has different effects on heart and skeletal muscle. *J Cachexia Sarcopenia Muscle* 9: 417–432, 2018.

51. **Kawahara Y**, **Yamaoka K**, **Iwata M**, **Fujimura M**, **Kajiume T**, **Magaki T**, **Takeda M**, **Ide T**, **Kataoka K**, **Asashima M**, **Yuge L**. Novel Electrical Stimulation Sets the Cultured Myoblast Contractile Function to 'On.' *Pathobiology* 73: 288–294, 2006.

52. **Faustino D**, **Brinkmeier H**, **Logotheti S**, **Jonitz-Heincke A**, **Yilmaz H**, **Takan I**, **Peters K**, **Bader R**, **Lang H**, **Pavlopoulou A**, **Pützer BM**, **Spitschak A**. Novel integrated workflow allows production and in-depth quality assessment of multifactorial reprogrammed skeletal muscle cells from human stem cells. *Cellular and Molecular Life Sciences* 79: 229, 2022.

53. **Kramer HF**, **Goodyear LJ**. Exercise, MAPK, and NF-κB signaling in skeletal muscle. *J Appl Physiol* 103: 388–395, 2007.

54. **Nedachi T**, **Fujita H**, **Kanzaki M**. Contractile C2C12 myotube model for studying exercise-inducible responses in skeletal muscle. *American Journal of Physiology-Endocrinology and Metabolism* 295: E1191–E1204, 2008.

55. **Raschke S**, **Eckardt K**, **Holven KB**, **Jensen J**, **Eckel J**. Identification and validation of novel contraction-regulated myokines released from primary human skeletal muscle cells. *PLoS One* 8: e62008, 2013.

56. **Peake JM**, **della Gatta P**, **Suzuki K**, **Nieman DC**. Cytokine expression and secretion by skeletal muscle cells: regulatory mechanisms and exercise effects. *Exerc Immunol Rev* 21: 8–25, 2015.

57. **Catoire M**, **Kersten S**. The search for exercise factors in humans. *The FASEB Journal* 29: 1615–1628, 2015.

58. **Miyatake S**, **Bilan PJ**, **Pillon NJ**, **Klip A**. Contracting C2C12 myotubes release CCL2 in an NF-κB-dependent manner to induce monocyte chemoattraction. *American Journal of Physiology-Endocrinology and Metabolism* 310: E160–E170, 2016.

59. **Huh JY**. The role of exercise-induced myokines in regulating metabolism. *Arch Pharm Res* 41: 14–29, 2018.

60. **Nedachi T**, **Hatakeyama H**, **Kono T**, **Sato M**, **Kanzaki M**. Characterization of contraction-inducible CXC chemokines and their roles in C2C12 myocytes. *American Journal of Physiology-Endocrinology and Metabolism* 297: E866–E878, 2009.

61. **Peake JM**, **Neubauer O**, **della Gatta PA**, **Nosaka K**. Muscle damage and inflammation during recovery from exercise. *J Appl Physiol* 122: 559–570, 2017.

833 62. **Koltai T**, **Reshkin SJ**, **Harguindey S**. *An innovative approach to understanding*
834 *and treating cancer: targeting ph: from etiopathogenesis to new therapeutic*
835 *avenues*. Academic Press, 2020.

836 63. **Jansen S**, **Pantaleon M**, **Kaye PL**. Characterization and regulation of
837 monocarboxylate cotransporters Slc16a7 and Slc16a3 in preimplantation mouse
838 embryos. *Biol Reprod* 79: 84–92, 2008.

839 64. **Brooks GA**. Lactate as a fulcrum of metabolism. *Redox Biol* 35: 101454, 2020.

840 65. **Wackerhage H**, **Vechetti IJ**, **Baumert P**, **Gehlert S**, **Becker L**, **Jaspers RT**, **de**
841 **Angelis MH**. Does a Hypertrophying Muscle Fibre Reprogramme its Metabolism
842 Similar to a Cancer Cell? [Online]. *Sports Medicine* 52: 2569–2578, 2022.
843 https://link.springer.com/10.1007/s40279-022-01676-1.

844 66. **Lawler JM**, **Rodriguez DA**, **Hord JM**. Mitochondria in the middle: exercise
845 preconditioning protection of striated muscle. *J Physiol* 594: 5161–5183, 2016.

846 67. **Scheele C**, **Nielsen S**, **Pedersen BK**. ROS and myokines promote muscle
847 adaptation to exercise. *Trends in Endocrinology & Metabolism* 20: 95–99, 2009.

848 68. **Fujita H**, **Mae K**, **Nagatani H**, **Horie M**, **Nagamori E**. Effect of hydrogen
849 peroxide concentration on the maintenance and differentiation of cultured skeletal
850 muscle cells. *J Biosci Bioeng* 131: 572–578, 2021.

851 69. **Liu L**, **Zhang Y**, **Liu T**, **Ke C**, **Huang J**, **Fu Y**, **Lin Z**, **Chen F**, **Wu X**, **Chen Q**.
852 Pyrroloquinoline quinone protects against exercise-induced fatigue and oxidative
853 damage via improving mitochondrial function in mice. *The FASEB Journal* 35:
854 e21394, 2021.

855 70. **Silva GJJ**, **Bye A**, **el Azzouzi H**, **Wisløff U**. MicroRNAs as Important Regulators
856 of Exercise Adaptation. *Prog Cardiovasc Dis* 60: 130–151, 2017.

857 71. **Soplinska A**, **Zareba L**, **Wicik Z**, **Eyileten C**, **Jakubik D**, **Siller-Matula JM**, **De**
858 **Rosa S**, **Malek LA**, **Postula M**. MicroRNAs as Biomarkers of Systemic Changes
859 in Response to Endurance Exercise—A Comprehensive Review. *Diagnostics* 10:
860 813, 2020.

861 72. **Vechetti IJ**, **Peck BD**, **Wen Y**, **Walton RG**, **Valentino TR**, **Alimov AP**, **Dungan**
862 **CM**, **Van Pelt DW**, **von Walden F**, **Alkner B**, **Peterson CA**, **McCarthy JJ**.
863 Mechanical overload-induced muscle-derived extracellular vesicles promote
864 adipose tissue lipolysis. *The FASEB Journal* 35, 2021.

865 73. **Rome S**, **Forterre A**, **Bouzakri K**, **Mizgier ML**. Skeletal muscle-released
866 extracellular vesicles: State of the art. *Front Physiol* 10: 929, 2019.

867 74. **Chen J-F**, **Mandel EM**, **Thomson JM**, **Wu Q**, **Callis TE**, **Hammond SM**,
868 **Conlon FL**, **Wang D-Z**. The role of microRNA-1 and microRNA-133 in skeletal
869 muscle proliferation and differentiation. *Nat Genet* 38: 228–233, 2006.

870 75. **Kim HK**, **Lee YS**, **Sivaprasad U**, **Malhotra A**, **Dutta A**. Muscle-specific
871 microRNA miR-206 promotes muscle differentiation. *J Cell Biol* 174: 677–687,
872 2006.

873 76. **Silver J**, **Wadley G**, **Lamon S**. Mitochondrial regulation in skeletal muscle: A role
874 for non-coding RNAs? *Exp Physiol* 103: 1132–1144, 2018.

875 77. **Rodrigues AC**, **Spagnol AR**, **Frias F de T**, **de Mendonça M**, **Araújo HN**,
876 **Guimarães D**, **Silva WJ**, **Bolin AP**, **Murata GM**, **Silveira L**. Intramuscular

Injection of miR-1 Reduces Insulin Resistance in Obese Mice. *Front Physiol* 12, 2021.

78. **Nie Y**, **Sato Y**, **Wang C**, **Yue F**, **Kuang S**, **Gavin TP**. Impaired exercise tolerance, mitochondrial biogenesis, and muscle fiber maintenance in miR-133a–deficient mice. *The FASEB Journal* 30: 3745–3758, 2016.

79. **Ma G**, **Wang Y**, **Li Y**, **Cui L**, **Zhao Y**, **Zhao B**, **Li K**. MiR-206, a Key Modulator of Skeletal Muscle Development and Disease. *Int J Biol Sci* 11: 345–352, 2015.

80. **Bydak B**, **Pierdoná TM**, **Seif S**, **Sidhom K**, **Obi PO**, **Labouta HI**, **Gordon JW**, **Saleem A**. Characterizing Extracellular Vesicles and Particles Derived from Skeletal Muscle Myoblasts and Myotubes and the Effect of Acute Contractile Activity [Online]. *Membranes (Basel)* 12: 464, 2022. https://www.mdpi.com/2077-0375/12/5/464.

81. **Everaert C**, **Luypaert M**, **Maag JL V.**, **Cheng QX**, **Dinger ME**, **Hellemans J**, **Mestdagh P**. Benchmarking of RNA-sequencing analysis workflows using whole-transcriptome RT-qPCR expression data. *Sci Rep* 7: 1559, 2017.

82. **Hawley JA**, **Lundby C**, **Cotter JD**, **Burke LM**. Maximizing Cellular Adaptation to Endurance Exercise in Skeletal Muscle. *Cell Metab* 27: 962–976, 2018.

83. **Farmawati A**, **Kitajima Y**, **Nedachi T**, **Sato M**, **Kanzaki M**, **Nagatomi R**. Characterization of contraction-induced IL-6 up-regulation using contractile C2C12 myotubes. *Endocr J* 60: 137–147, 2013.

84. **Shirasaki Y**, **Yamagishi M**, **Suzuki N**, **Izawa K**, **Nakahara A**, **Mizuno J**, **Shoji S**, **Heike T**, **Harada Y**, **Nishikomori R**. Real-time single-cell imaging of protein secretion. *Sci Rep* 4: 4736, 2014.

900 85. **Russell AP**, **Lamon S**, **Boon H**, **Wada S**, **Güller I**, **Brown EL**, **Chibalin A v.**,
901 **Zierath JR**, **Snow RJ**, **Stepto N**, **Wadley GD**, **Akimoto T**. Regulation of miRNAs
902 in human skeletal muscle following acute endurance exercise and short-term
903 endurance training. *J Physiol* 591: 4637–4653, 2013.

904 86. **Tarum J**, **Folkesson M**, **Atherton PJ**, **Kadi F**. Electrical pulse stimulation: an in
905 vitro exercise model for the induction of human skeletal muscle cell hypertrophy. A
906 proof-of-concept study. *Exp Physiol* 102: 1405–1413, 2017.

907 87. **Shi J**, **Zhang Y**, **Tan D**, **Zhang X**, **Yan M**, **Zhang Y**, **Franklin R**, **Shahbazi M**,
908 **Mackinlay K**, **Liu S**, **Kuhle B**, **James ER**, **Zhang L**, **Qu Y**, **Zhai Q**, **Zhao W**,
909 **Zhao L**, **Zhou C**, **Gu W**, **Murn J**, **Guo J**, **Carrell DT**, **Wang Y**, **Chen X**, **Cairns**
910 **BR**, **Yang X**, **Schimmel P**, **Zernicka-Goetz M**, **Cheloufi S**, **Zhang Y**, **Zhou T**,
911 **Chen Q**. PANDORA-seq expands the repertoire of regulatory small RNAs by
912 overcoming RNA modifications. *Nat Cell Biol* 23: 424–436, 2021.

913

914 **FIGURE LEGENDS**

915 **FIGURE 1.** Schematic presentation of the study design.

916 **FIGURE 2.** The effects of exercise-like electrical pulse stimulation (EL-EPS, EPS in the figure)
917 and media glucose availability on the C2C12 myotube transcriptome. (A) Venn graph of the
918 differentially expressed genes (DEGs). (B) Principal component analysis (PCA) of the DEGs.
919 The read counts were used to create the PCA score plot. The heat map categorization of the
920 DEGs after EL-EPS in (C) low and (D) high glucose (LG and HG, respectively) condition as
921 well as (E) in the pool of the stimulated vs. non-stimulated samples (EPS vs. CTRL). The dashed
922 lines cluster the DEGs that respond similarly to EL-EPS in each comparison. The heat map
923 categorization is based on *k*-means clustering and the coloring on the *z*-scores. In A, false
924 discovery rate < 0.05 and fold change > $\left|1.2\right|$. N = 5 per group except in EPS vs. CTRL, N =
925 10 per group.

926 **FIGURE 3**. Complementary analysis of the mRNA-seq results after exercise-like electrical pulse
927 stimulation (EL-EPS, EPS in the figure) by RT-qPCR. The mRNA expression of (A) *Cxcl1*, (B)
928 *Cxcl5*, (C) *Tceal7*, and (D) *Scml4*. For the analysis of EL-EPS and media glucose content (EPS
929 and HG main effects, respectively) and their interaction effect, the two-way MANOVA was
930 used. The group comparisons were analyzed with multivariate Tukey´s test. In the figures, the
931 values are presented as normalized to low glucose (LG) = 1 or high glucose (HG) = 1. N = 3–4
932 per group. * = P < 0.05 and *** = P < 0.001, respectively.

933 **FIGURE 4.** The top ten (A) over- and (B) underrepresented pathways after exercise-like
934 electrical pulse stimulation (EL-EPS, EPS in the figure) on the C2C12 myotubes. The
935 bioinformatic gene set enrichment analysis (GSEA) pathway analyses were conducted by using
936 Gene Ontology Biological Processes (GOPB) database. Data in the figures is categorized by
937 normalized enrichment scores (NES) and -Log10 of false discovery rate (FDR) values. Note that
938 FDR < 0.05 equals >1.3 in -Log10 (FDR) scale and for clarity, the X- and Y-axes do not start at
939 zero for the plots. Bold = pathway related to contractility and/or muscle structure, italics =

pathway related to cytokine and other inflammatory responses. N = 5 per group except for a pool of stimulated vs. non-stimulated (EPS vs. CTRL) comparison, N = 10 per group.

FIGURE 5. The effects of the exercise-like electrical pulse stimulation (EL-EPS, EPS in the figure) and media glucose content on cytokine and inflammatory signaling as well as on contractile protein. (A) Phosphorylated NF-κB^{Ser536}, (B) phosphorylated STAT3^{Tyr705} and total STAT3, (C) CCL2 and (D) myosin heavy chain 1 (MF 20). (E) Representative blots. −, no stimulation; +, stimulation. In the figures, the values are presented as normalized to low glucose (LG) = 1 or high glucose (HG) = 1. The two-way MANOVA was used to analyze EL-EPS and media glucose content effects (EPS and HG main effects, respectively) and their interaction effect, whereas group comparisons were analyzed with multivariate Tukey's test. N = 6 per group.

FIGURE 6. The effects of the exercise-like electrical pulse stimulation (EL-EPS, EPS in the figure) on the extracellular vesicle (EV) microRNA (miRNA) content. A) Top 10 miRNAs in the C2C12 cell-derived EVs based on small RNA sequencing. The proportions represent the percentage of the top 50 miRNAs analyzed. All four groups were pooled for the analysis. B) The heat map categorization of the EV-derived miRNAs in the pool of the high and low glucose samples (HG vs. LG, respectively). The dashed line clusters the miRNAs that respond similarly to the media glucose content. The heat map categorization is based on *k*-means clustering and the coloring on the *z*-scores. The expression of (C) miR-1-3p, (D) miR-206-3p and (E) miR-133a-3p analyzed by RT-qPCR. The values are presented as normalized to LG or HG = 1. In B, the two-way MANOVA was used to analyze EL-EPS and media glucose content effects (EPS and HG main effects, respectively) and their interaction effect, whereas group comparisons were analyzed with multivariate Tukey's test. In C-D, EPS and HG effects as well as the group comparisons were conducted using Mann Whitney *U*-test. In A, N = 20, in B, N = 10 per group (HG vs. LG) and in C-E, N = 5–6 per group.

EXPERIMENTS & COMPARISONS

±EL-EPS (24h, 1 Hz, 2 ms, 12 V)

LG 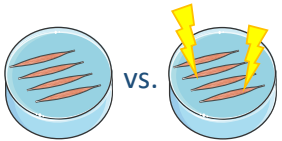 vs.

HG 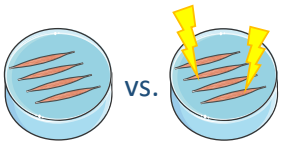 vs.

Low (LG, 1g/L) OR high (HG, 4.5 g/L) glucose media

COLLECTION

Myotubes Media

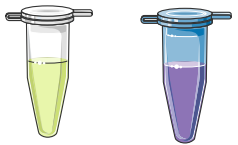

RNA, proteins

EVs

ANALYSES

Myotube mRNA seq (N = 5)

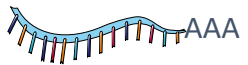

Myotube RT-qPCR (N = 3-4)

EV sRNA seq (N = 5)
EV miRNA RT-qPCR (N = 5-6)

Myotube Western blot (N = 6)

A

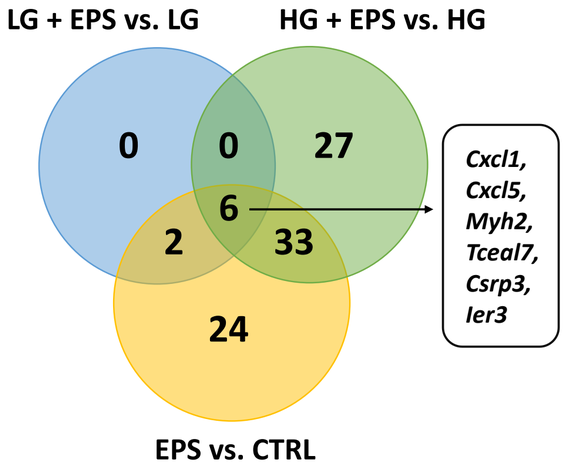

B

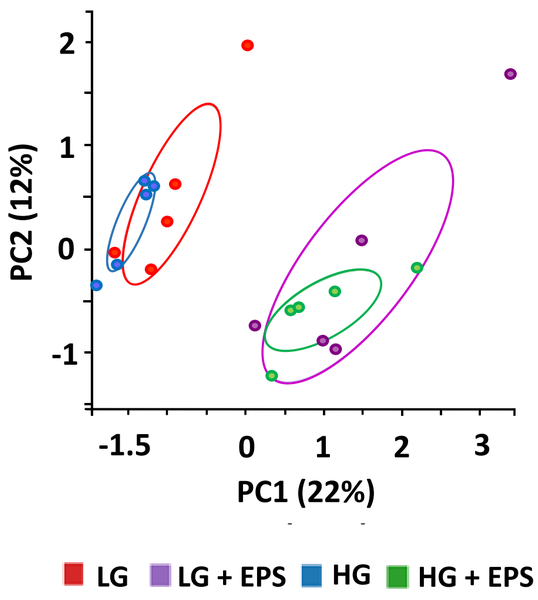

C

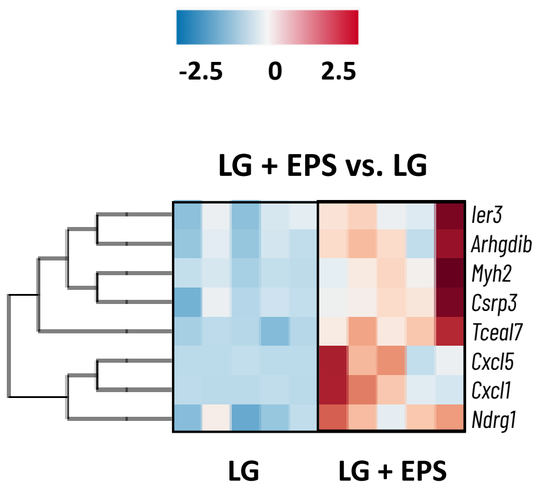

D

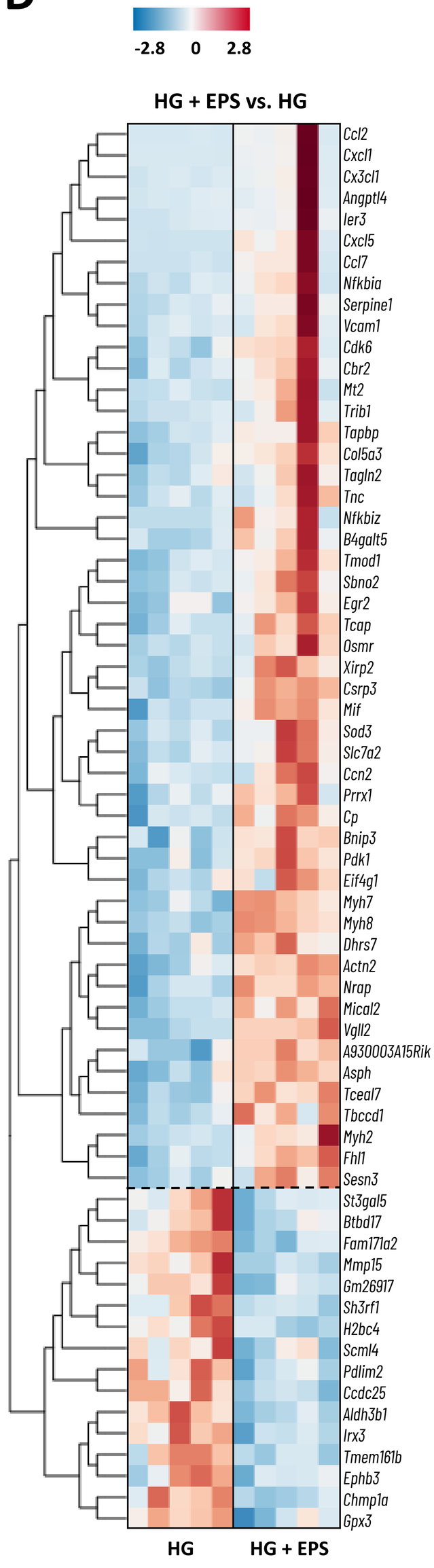

E

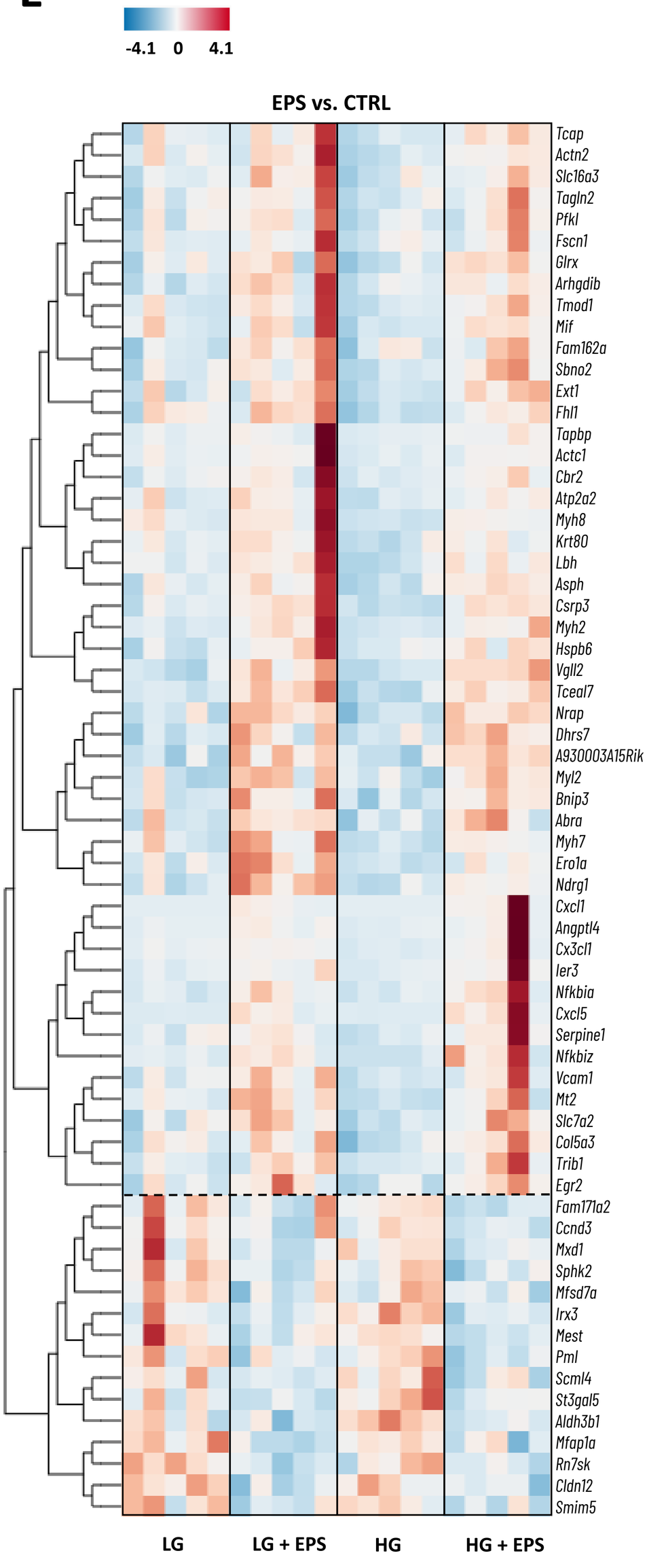

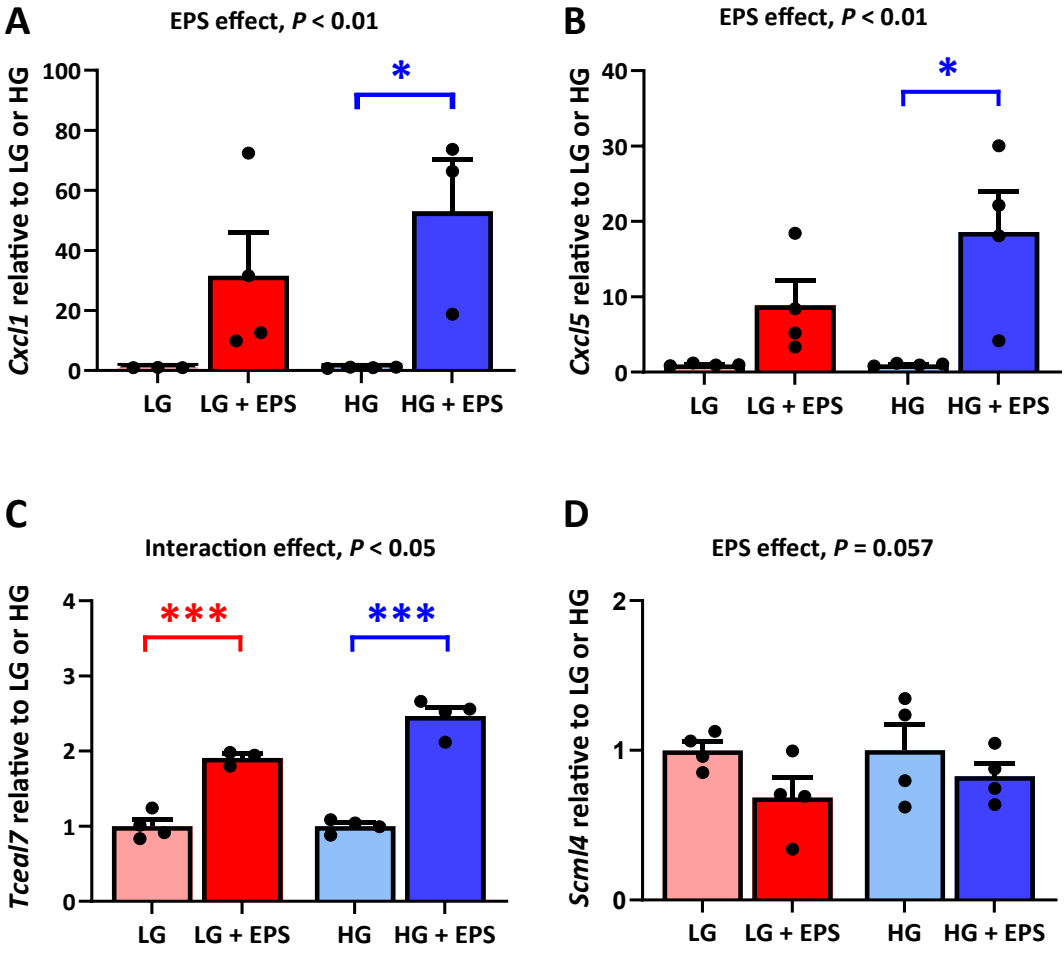

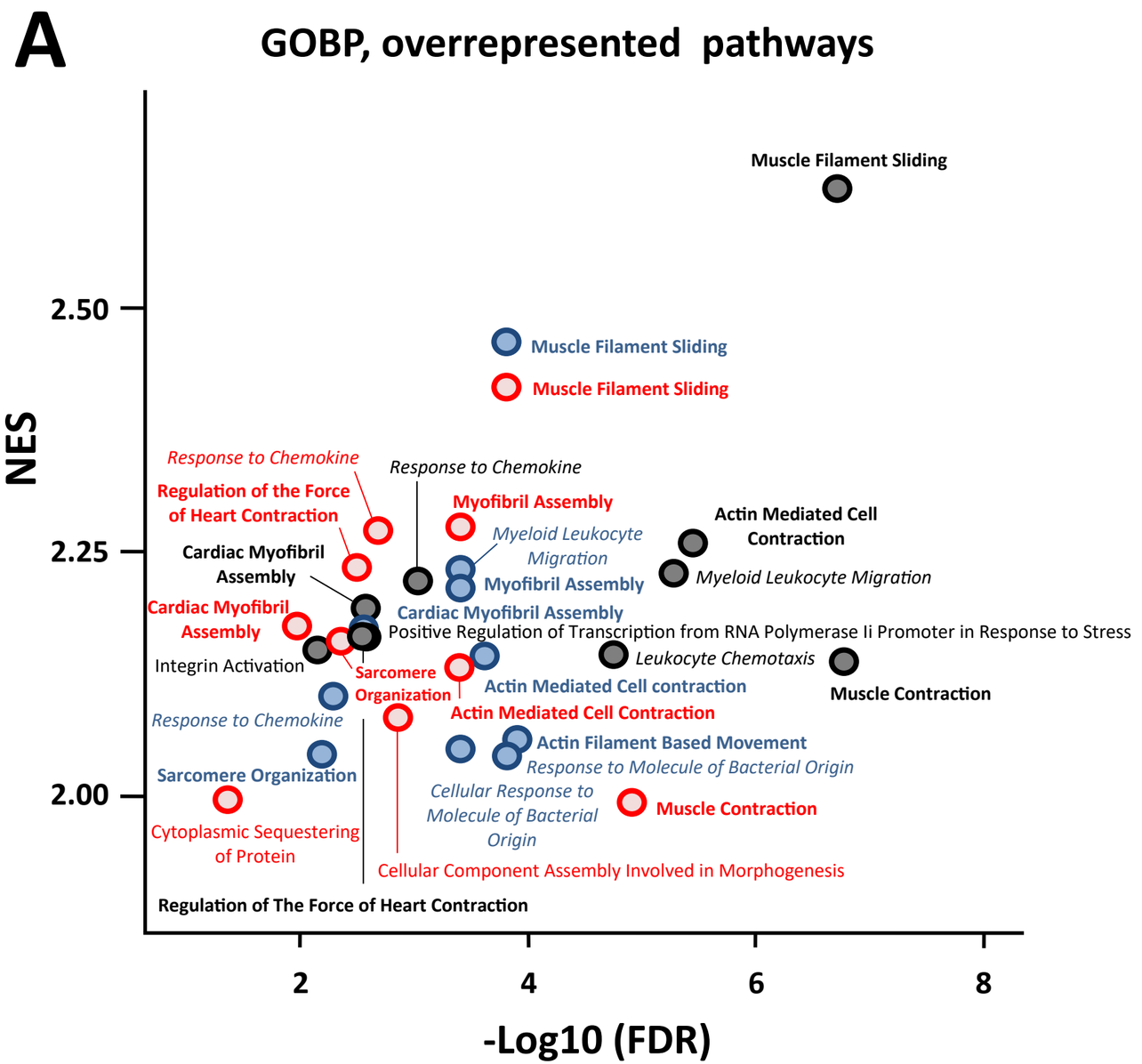

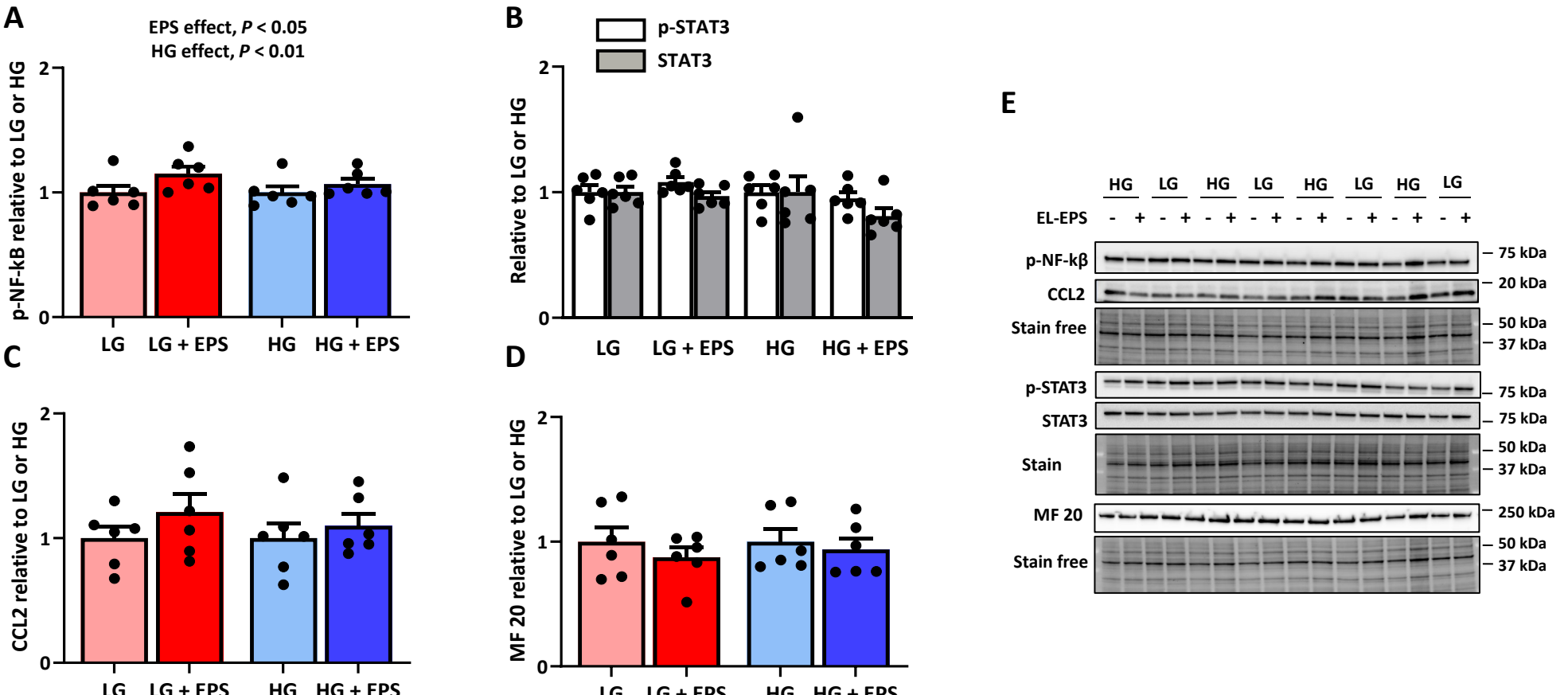

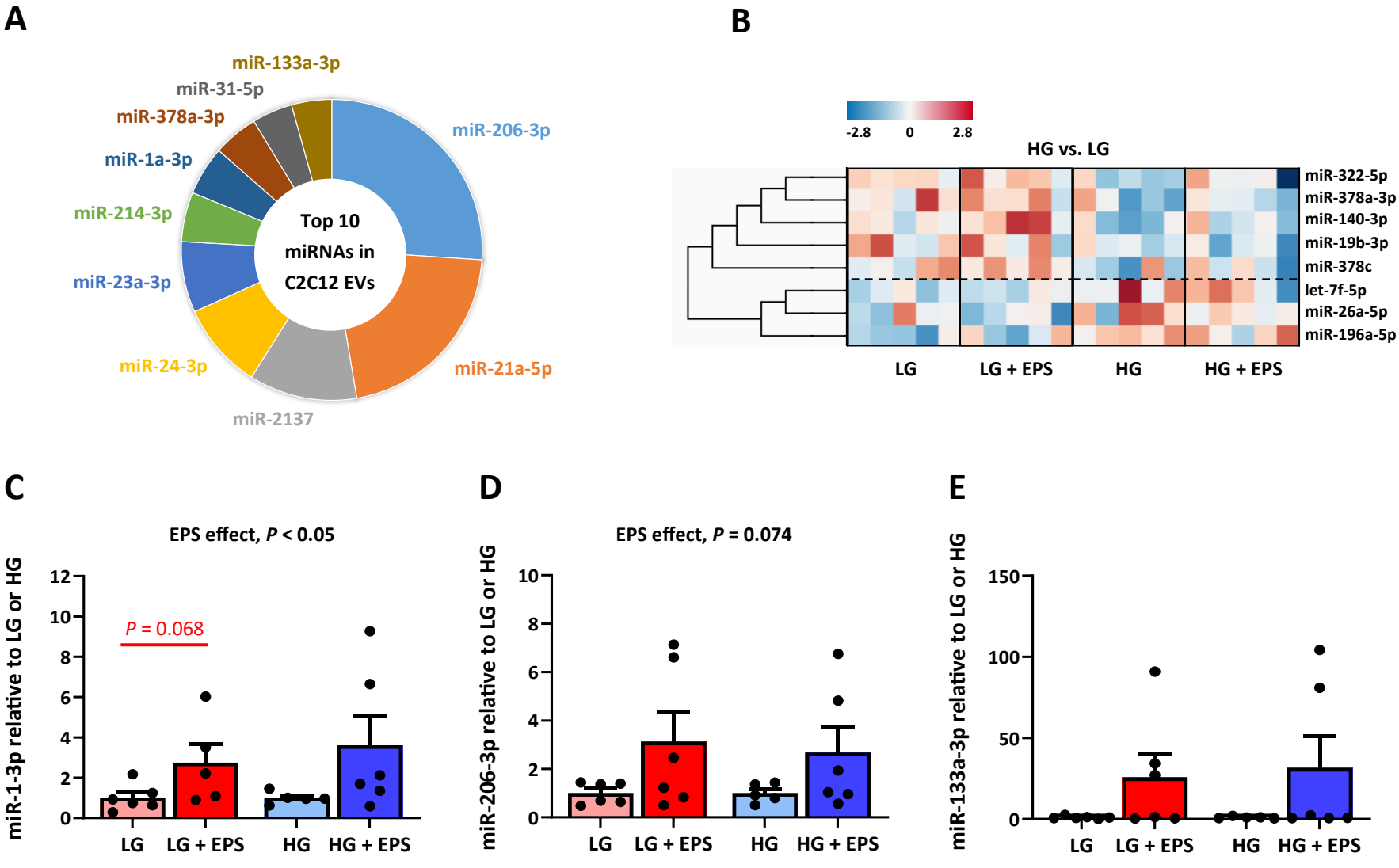

Higher glucose availability augments transcriptional responses but not miR-1-3p packing into extracellular vesicles in the contracting C2C12 myotubes

High (4.5 g/l) OR low (1 g/l) glucose media

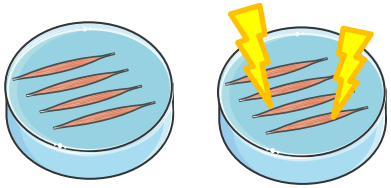

± 24h, 1 Hz, 2 ms, 12 V electrical pulse stimulation

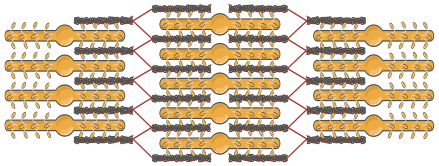

Genes related to contractility

↑ ↑ / ↑

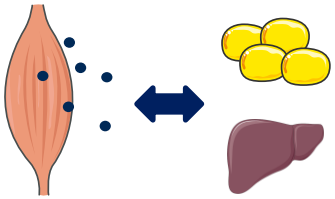

Genes related to cytokine and inflammatory response

↑ ↑ / ↑

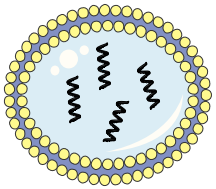

miR-1-3p packing into extracellular vesicles

↑ / ↑

CONCLUSION: Independent of glucose availability, myotube contractions promote packing of miR-1-3p into extracellular vesicles thus supporting its´ role as a potential exerkine